Preparation of Porous Collagen Scaffolds Using Template Method for Cartilage Tissue Engineering

Yan Xie

February 2022

Preparation of Porous Collagen Scaffolds Using Template Method for Cartilage Tissue Engineering

Yan Xie

Doctoral Program in Materials Science and Engineering

Submitted to the Graduate School of

Pure and Applied Sciences

in Partial Fulfillment of the Requirements

for the Degree of Doctor of Philosophy in

Engineering

at the

University of Tsukuba

Contents

List of abbreviations

PLGA	Poly($_{L,D}$-lactic-*co*-glycolic acid)
ECM	Extracellular matrix
hMSCs	Human mesenchymal stem cells
RGD	Arg-Gly-Asp
DMEM	Dulbecco's modified eagle medium
DNA	Deoxyribonucleic acid
RT-PCR	Real-time polymerase chain reaction
GAPDH	Glyceraldehyde-3-phosphate dehydrogenase
FBS	Fetal bovine serum
sGAG	Sulfated glycosaminoglycan
HE	Hematoxylin and eosin
TGF-β3	Transforming growth factor-beta3
RNA	Ribonucleic acid
PBS	Phosphate buffer saline
cDNA	Complementary DNA
BACs	Bovine articular chondrocytes
MSCGMTM	Mesenchymal stem cell growth medium
RT-PCR	Real-time polymerase chain reaction
DAPI	4′,6-diamidino-2-phenylindole dihydrochloride
Col	Collagen
ITS	ITS+1 (Insulin, transferrin, sodium selenite + linoleic acid) liquid media supplement
3D	Three-dimensional

Chapter 1

General introduction

Articular cartilage is a connective tissue which has avascular, aneural and alymphatic characteristics [1]. It is composed of a large amount of extracellular matrix (ECM) and sparsely distributed chondrocytes [2-4]. The main components of ECM are collagen type II and proteoglycans, which provide compressive strength and tensile strength (Figure 1.1) [5-7]. Chondrocytes maintain low metabolic activities in mature cartilage tissue, which leads to the slow turnover of matrix and low self-repair capacity [8-11]. Cartilage injuries occur due to trauma and degenerative pathologies, which result in joint pain, bone-to-bone contact and loss of joint function [12, 13]. Currently, surgical treatments, such as microfracture, mosaicplasty and tissue engineering strategies, have been broadly used to repair articular cartilage defects [14-16].

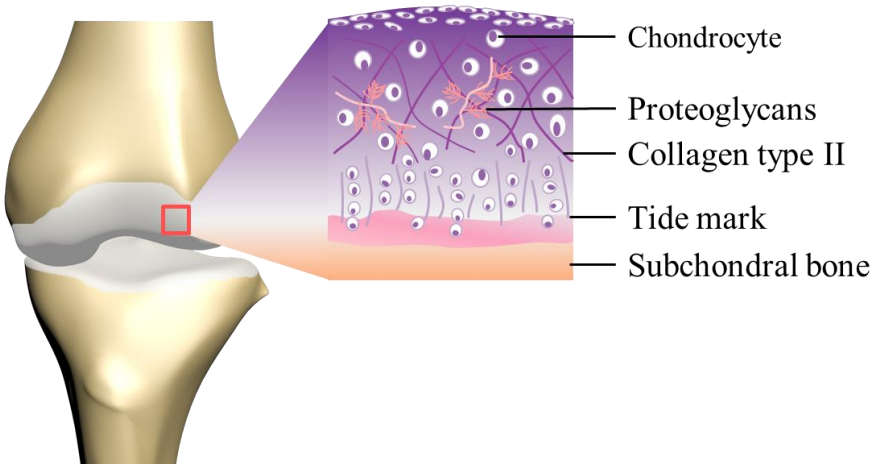

Figure 1.1 Structure and composition of articular cartilage.

1.1 Current treatments of articular cartilage defects

1.1.1 Microfracture

Microfracture surgery is a technique used to treat small cartilage lesions by stimulation of bone marrow (Figure 1.2) [15, 17, 18]. The awl is used to create channels from the debrided cartilage defect to subchondral bone. During this process, bone marrow is released from the cavity of the bone to cartilage defect area and forms blood clots [19]. It stimulates the migration of mesenchymal stem cells (MSCs), which results in the formation of fibrocartilage regenerative tissue [2, 20, 21]. Compared with hyaline cartilage, the fibrocartilage has inferior biomechanical, biochemical and durability[5, 22]. Many studies have reported initial functional improvement within 2 years after surgery [19, 23, 24]. However, typical deterioration of initial clinical

improvement has been observed during long-term follow-up after microfracture treatment [25, 26].

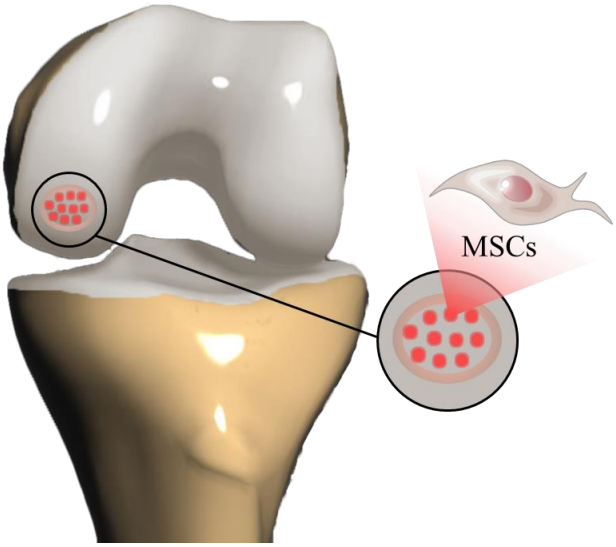

Figure 1.2 Microfracture technique for articular cartilage regeneration.

1.1.2 Mosaicplasty

Mosaicplasty is usually applied for young patients with small or medium osteochondral defects [16, 27]. Osteochondral plugs are harvested from relatively low-weight-bearing regions of cartilage and transplanted to the chondral or osteochondral defect areas [28-31]. In order to maintain chondrocyte viability and remodel a smooth cartilage surface, the small size of osteochondral plugs is needed for success of the procedure [27, 32, 33]. Mosaicplasty technique transfers osteochondral units to chondral defects, which can bear compressive loads in the early postoperative period [34, 35]. The availability of osteochondral grafts and morbidity of donor sites remain as the limitations of mosaicplasty [36].

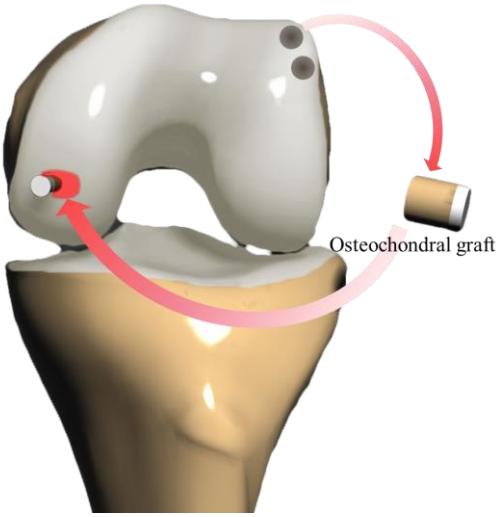

Figure 1.3 Illustration of mosaicplasty technique. Osteochondral autograft is transferred from the low-weight bearing regions of the knee to the cartilage defect.

1.1.3 Autologous chondrocyte implantation

Due to the limitations of traditional treatments, such as microfracture and mosaicplasty, cell-based cartilage tissue engineering has been developed to treat cartilage lesions [14, 37-39]. Autologous chondrocyte implantation (ACI) has been approved by US Food and Drug Administration (FDA), which is regarded as a treatment for large defects [40-42]. A small cartilage biopsy is harvested using biopsy punch from a low-weight-bearing region of the knee and enzymatically digested to obtain chondrocytes during the first surgery [1, 2, 18, 21]. Chondrocytes are expanded *in vitro* to increase cell number, implanted into the debrided cartilage lesion and covered with a membrane during the second arthroscopic operation [43]. ACI has two major advantages: it avoids causing a potential immune response or viral infections from allogeneic chondrocytes by using patients' cells; unlike mosaicplasty, the small amount of cartilage tissue biopsy for ACI minimizes the morbidity of the donor site [15, 17, 44, 45]. However, the implantation of autologous chondrocytes in suspension and the following operation by covering cartilage defect with a membrane may lead to uneven chondrocyte distribution and potential cell leakage [46, 47].

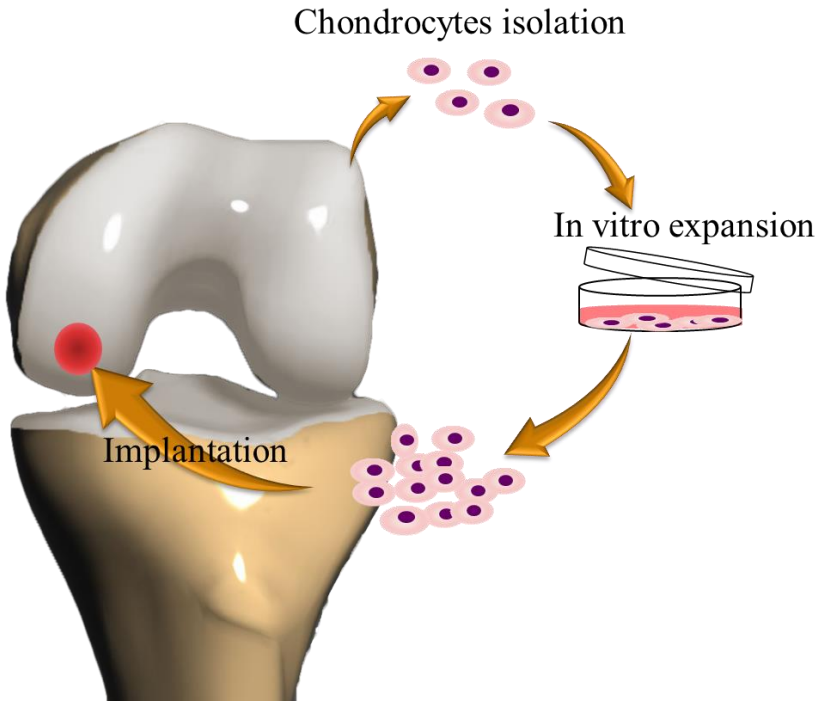

Figure 1.4 Autologous chondrocyte implantation involves chondrocytes isolation, *in vitro* expansion and cell implantation.

1.1.4 Scaffold-based tissue engineering

To address the problems of autologous chondrocyte implantation, 3D scaffolds are used to deliver chondrocytes into the cartilage defects (Figure 1.5) [48-50]. Cells are seeded into the scaffolds before implantation, which has improved surgical handling [51-53]. 3D scaffolds can support chondrocyte proliferation, guide the synthesis of cartilaginous extracellular matrix synthesis and the formation of engineering tissue [49, 54-57]. There are some advantages of scaffold-based tissue engineering. Firstly, it is possible to design the shape of scaffold to fill the defects with irregular shape using the scaffold-based approach compared with mosaicplasty and autologous chondrocyte implantation [58, 59]. Secondly, due to the introduction of supportive scaffold, the postoperative recovery time can be shortened and better outcome can

be achieved [21, 60]. Thirdly, chondrocytes are more prone to maintain phenotype and capacity to produce cartilaginous ECM when they are cultured in a 3D scaffold [47, 61-64].

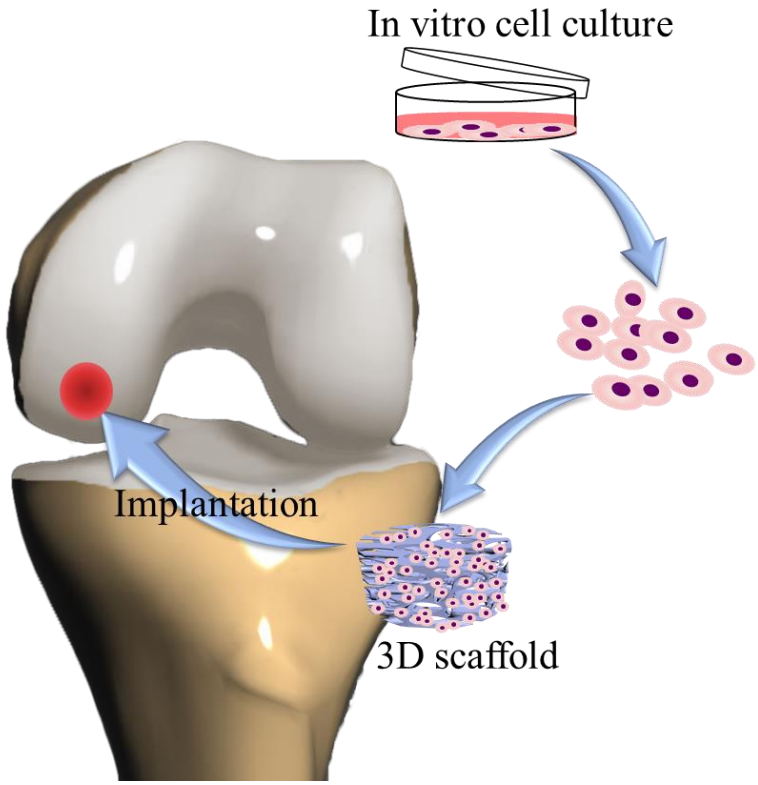

Figure 1.5 Scaffold-based cartilage tissue engineering combines cells and 3D supportive scaffold before implantation.

1.2 3D scaffolds for tissue engineering

1.2.1 Basic requirements of scaffolds

Scaffold plays a pivotal role in tissue engineering since it can regulate cell functions and guide the formation of regenerated tissue [50, 60, 65-67]. In tissue engineering, 3D scaffold acts as a temporary replacement of extracellular matrix, which creates a permissive environment to support cell attachment, proliferation, differentiation and ECM deposition [66, 68-70]. An ideal scaffold should meet the following basic requirements:

I. Biocompatibility

The first criterion of scaffold is biocompatibility. A scaffold should support cellular activities, such as adhesion, migration and proliferation [71-73]. After implantation, scaffold and its degradation products should not cause local or systemic negative side effects in the body [74-78].

II. Degradability

The purpose of tissue engineering is to promote cell proliferation and ECM secretion to regenerate tissues with the support of scaffolds [79, 80]. During the regeneration process, the scaffold is gradually degraded, absorbed by the body, and eventually replaced by neotissue [81-89]. Therefore, scaffolds must be degradable and the degradation rate should meet the regeneration rate of neotissue to achieve good structural integrity of

tissue [90-92].

III. Mechanical properties

Ideally, scaffold should have suitable mechanical property to allow surgical handling and maintain the shape during *in vitro* culture and implantation [70, 81, 93-95]. The appropriate mechanical properties of scaffolds vary among different tissues [81, 96-102]. The efforts to obtain good mechanical properties by decreasing the porosity have failed due to the inadequate tissue ingrowth [103, 104]. The balance between mechanical property and porosity is the key for the design and preparation of scaffold [105].

IV. Scaffold architecture

The porous structure is important to the success of tissue engineering [106-109]. Scaffolds with interconnected porous structure and appropriate porosity allow cellular penetration and sufficient supply of nutrients [110-113]. Interconnected pores in the scaffold can promote homogenous cell distribution and the formation of homogenous tissue [112, 114-118]. In addition, the interconnected structure is also beneficial for the diffusion of degradation products and wastes avoiding the interference of surrounding tissues [101, 119-122].

The pore size is another important parameter of scaffold. The pores in the scaffold should be large enough for cell penetration and migration while providing high specific surface for cell adhesion and proliferation [123-128]. The optimum pore size varies depending on different cell types and tissues, which can affect cell functions [129].

1.2.2 Techniques for porous scaffold fabrication

Numerous methods have been developed to fabricate porous scaffold for the application of tissue engineering. Ideally, the scaffold should have appropriate porosity, pore size, high specific surface area and interconnectivity, which provide suitable environment to sustain cell functions [130]. The most frequently used methods for the porous scaffold fabrication are shown as follows.

1.2.2.1 Particulate leaching technique

In this technique, the polymer melt or solution is mixed with porogen particulates. The polymer/particulates mixture is solidified and then the particulates are leached to form porous structures (Figure 1.6) [97, 131-135].

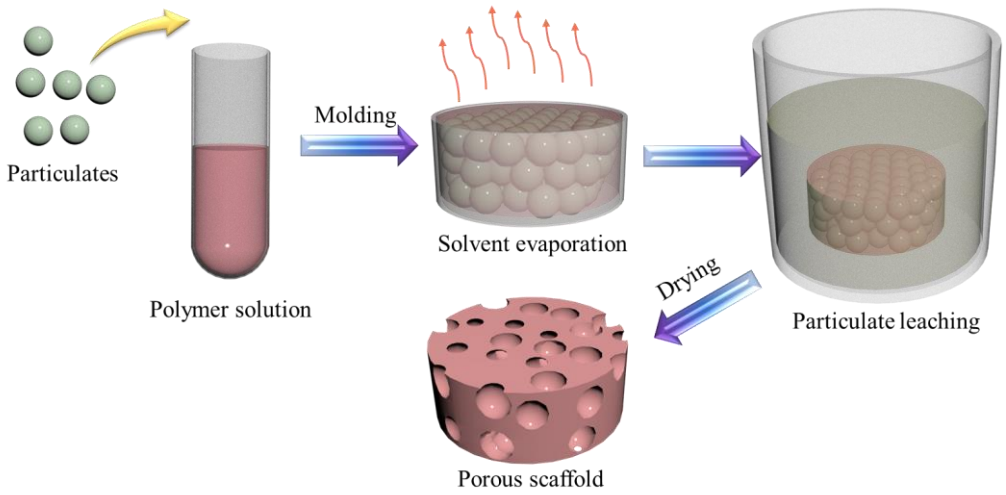

Figure 1.6 Particulate leaching technique.

Scaffold is obtained by selectively leaching the particulates. The sacrificial agents, such as salt particles, gelatine beads, paraffine beads and polystyrene microspheres can be used as porogens. The pore size, shape and porosity can be controlled by the size of particulates and the ratio of polymer and particulates[110, 136, 137]. This method is easy to carry out and cost-effective. However, particulate leaching may result in the formation of closed pores in the scaffolds[138].

1.2.2.2 Electrospinning

Electrospinning is a process to fabricate nonwoven fabric products (Figure 1.7) [94, 139, 140]. The polymer solution is injected into a capillary tube and forms a polymer solution droplet. During the electrospinning process, a strong electric field is applied and an electric charge is induced on the surface of polymer solution. Once the repulsive electrical forces overcome the surface tension forces, the polymer solution jet is ejected from the tip to the collector. The jet passes through the air condition, resulting in the evaporation of solvent. Eventually, nonwoven polymer fabric scaffold is formed on the collector [91, 141-145]. The size and morphology of fibers can be affected by the molecular weight, concentration and conductivity of polymer, voltage, collector-to-needle tip distance and humidity [146]. However, the small pores formation in the electrospinning scaffolds hinders the cellular infiltration into the scaffolds [6].

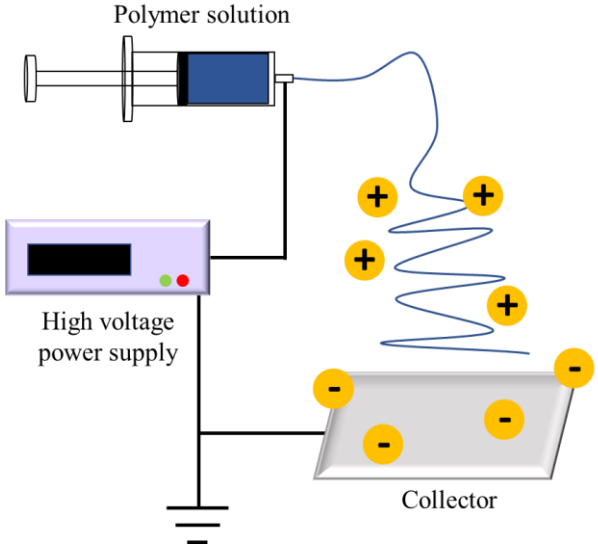

Figure 1.7 Electrospinning device

1.2.2.3 Foaming

Foaming technique combines polymers and gas to fabricate porous scaffolds. Traditional foaming technique uses foaming agent to form gas bubbles in the polymer matrix [147-150]. However, the residue of pore-forming agents may be toxic to cells. Supercritical fluid foaming has been developed to generate pores using a fluid state of carbon dioxide (CO_2) (Figure 1.8) [121, 151]. This method can fabricate porous scaffold without using pore-forming agents and organic solvents [121, 148, 152, 153]. The disadvantages of foaming include the closed pore structures and dense polymeric skin layers.

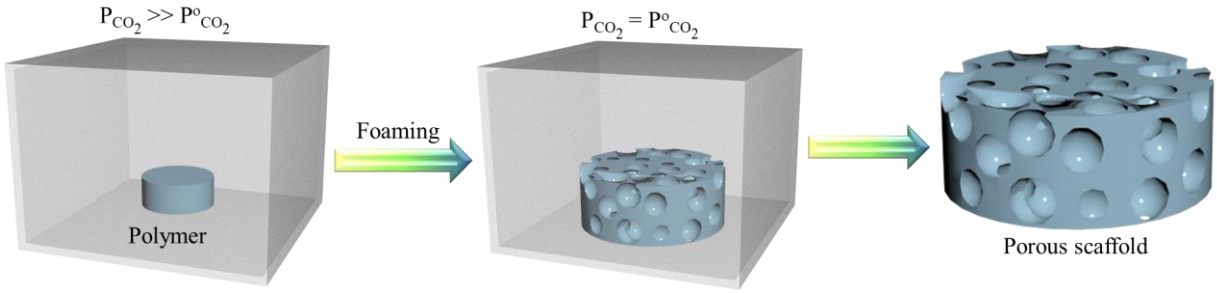

Figure 1.8 Supercritical fluid foaming method.

1.2.2.4 Freeze-drying

The polymers are dissolved in an appropriate solvent, such as water and organic solvents, and cooled under the freezing point. The ice crystals of the solvent are formed and served as porogens, which control the pore size of porous scaffolds by controlling temperature and polymer concentration [154]. The frozen solvent crystals are evaporated by sublimation under a negative pressure condition to prepare a scaffold with porous structures [155]. Freeze-drying is a quick and efficient technique to prepare 3D porous scaffolds, which can keep the activity of the integrated bioactive factors. The disadvantage of this technique is the generation of small and irregular pores.

1.3 Motivation, objective and outline

1.3.1 Motivation

Pore interconnectivity is required for scaffolds in the application of tissue engineering. Lack of pore interconnectivity will lead to nonhomogeneous cell distribution in the scaffold and eventually result in the defects in the engineered tissues. Many methods have been developed to fabricate 3D porous scaffolds, such as solvent casting/particle leaching, electrospinning, foaming, phase separation and freeze-drying. These methods are difficult to generate interconnected pores. In recent years, some methods have been developed to improve pore interconnectivity. Sphere templating technique is employed to prepare porous scaffold by using specific temperature to sinter spheres as templates. After removing the templates, the interconnections are formed between two adjacent pores. Microfluidic approach is employed to produce scaffolds with interconnected porous structures. These methods may lead to local deficiency of the pore structures resulting in void regions in the engineered tissue.

Although attempts have been made to improve the interconnectivity of porous scaffold for tissue engineering, it is still difficult to prepare a scaffold with integral and continuous interconnected porous structures. A method to prepare scaffold with well interconnected porous structure is desirable.

1.3.2 Objective and outline

In order to prepare scaffold with well-interconnected porous structure for cartilage tissue engineering, a porous template prepared by solution casting and particle leaching method was used to produce porous scaffolds with interconnected pore structures.

In chapter 2, poly(D,L-lactide-co-glycolide) (PLGA) sponges were used as sacrificial templates to control the interconnectivity of collagen scaffolds. The interconnected porous structures of collagen scaffolds using

porous PLGA sponges with different porosities and pore sizes were prepared and investigated.

In chapter 3, bovine articular chondrocytes were cultured in the collagen scaffolds prepared in chapter 2 to investigate the influence of their pore structures on cell distribution, cell proliferation, matrix secretion and cartilage tissue regeneration.

In chapter 4, the collagen scaffolds were used for 3D culture of human bone marrow-derived MSCs (hMSCs) to investigate their effects on chondrogenic differentiation of hMSCs. In addition, the hMSCs/scaffold constructs were subcutaneously implanted into nude mice to evaluate the *in vivo* formation of cartilaginous tissue.

In chapter 5, all the results are summarized.

1.4 References

[1] W. Wei, H. Dai, Articular cartilage and osteochondral tissue engineering techniques: Recent advances and challenges, Bioactive materials 6(12) (2021) 4830-4855.
[2] H. Kwon, W.E. Brown, C.A. Lee, D. Wang, N. Paschos, J.C. Hu, K.A. Athanasiou, Surgical and tissue engineering strategies for articular cartilage and meniscus repair, Nature Reviews Rheumatology 15(9) (2019) 550-570.
[3] J. Malda, J. Groll, P.R. van Weeren, Rethinking articular cartilage regeneration based on a 250-year-old statement, Nat Rev Rheumatol 15(10) (2019) 571-572.
[4] R.E. Wilusz, J. Sanchez-Adams, F. Guilak, The structure and function of the pericellular matrix of articular cartilage, Matrix Biology 39 (2014) 25-32.
[5] A.R. Armiento, M. Alini, M.J. Stoddart, Articular fibrocartilage - Why does hyaline cartilage fail to repair?, Adv Drug Deliv Rev 146 (2019) 289-305.
[6] Mechanical Properties and Cellular Proliferation of Electrospun Collagen Type II, Tissue engineering 10(9-10) (2004) 1510-1517.
[7] Y. Shi, X. Hu, J. Cheng, X. Zhang, F. Zhao, W. Shi, B. Ren, H. Yu, P. Yang, Z. Li, Q. Liu, Z. Liu, X. Duan, X. Fu, J. Zhang, J. Wang, Y. Ao, A small molecule promotes cartilage extracellular matrix generation and inhibits osteoarthritis development, Nat Commun 10(1) (2019) 1914.
[8] A. Gigante, C. Bevilacqua, C. Zara, M. Travasi, C. Chillemi, Autologous chondrocyte implantation: cells phenotype and proliferation analysis, Knee Surgery, Sports Traumatology, Arthroscopy 9(4) (2001) 254-8.
[9] T.B.F. Woodfield, S. Miot, I. Martin, C.A. van Blitterswijk, J. Riesle, The regulation of expanded human nasal chondrocyte re-differentiation capacity by substrate composition and gas plasma surface modification, Biomaterials 27(7) (2006) 1043-1053.
[10] Z. Zhao, C. Fan, F. Chen, Y. Sun, Y. Xia, A. Ji, D.A. Wang, Progress in Articular Cartilage Tissue Engineering: A Review on Therapeutic Cells and Macromolecular Scaffolds, Macromolecular Bioscience 20(2) (2020) e1900278.
[11] B.G. Sengers, H.K. Heywood, D.A. Lee, C.W. Oomens, D.L. Bader, Nutrient utilization by bovine articular chondrocytes: a combined experimental and theoretical approach, Journal of Biomechanical Engineering 127(5) (2005) 758-66.
[12] R. Suppanee, M. Yazdifar, M. Chizari, I. Esat, N.V. Bardakos, R.E. Field, Simulating osteoarthritis: the effect of the changing thickness of articular cartilage on the kinematics and pathological bone-to-bone contact in a hip joint with femoroacetabular impingement, European Orthopaedics and Traumatology 5(1) (2014) 65-73.
[13] J.E.J. Bekkers, L.B. Creemers, W.J.A. Dhert, D.B.F. Saris, Review: Diagnostic Modalities for Diseased Articular Cartilage-From Defect to Degeneration: A Review, CARTILAGE 1(3) (2010) 157-164.
[14] T. Negoro, Y. Takagaki, H. Okura, A. Matsuyama, Trends in clinical trials for articular cartilage repair by cell therapy, NPJ Regen Med 3 (2018) 17.
[15] D.B.F. Saris, J. Vanlauwe, J. Victor, K.F. Almqvist, R. Verdonk, J. Bellemans, F.P. Luyten, Treatment of Symptomatic Cartilage Defects of the Knee:Characterized Chondrocyte Implantation Results in Better Clinical Outcome at 36 Months in a Randomized Trial Compared to Microfracture, The American Journal of Sports Medicine 37(1_suppl) (2009) 10-19.
[16] E. Solheim, J. Hegna, E. Inderhaug, Long-Term Survival after Microfracture and Mosaicplasty for Knee Articular Cartilage Repair: A Comparative Study Between Two Treatments Cohorts, CARTILAGE 11(1) (2018) 71-76.
[17] D.B.F. Saris, J. Vanlauwe, J. Victor, M. Haspl, M. Bohnsack, Y. Fortems, B. Vandekerckhove, K.F. Almqvist, T. Claes, F. Handelberg, K. Lagae, J. van der Bauwhede, H. Vandenneucker, K.G.A. Yang, M. Jelic, R. Verdonk, N. Veulemans, J. Bellemans, F.P. Luyten, Characterized Chondrocyte Implantation Results in Better Structural Repair when Treating Symptomatic Cartilage Defects of the Knee in a Randomized Controlled Trial versus Microfracture, The American Journal of Sports Medicine 36(2) (2008) 235-246.
[18] M. Chimutengwende-Gordon, J. Donaldson, G. Bentley, Current solutions for the treatment of chronic articular cartilage defects in the knee, EFORT Open Rev 5(3) (2020) 156-163.
[19] J.R. Steadman, W.G. Rodkey, J.J. Rodrigo, Microfracture: Surgical Technique and Rehabilitation to Treat Chondral Defects, Clinical Orthopaedics and Related Research® 391 (2001) S362-S369.
[20] S. Jiang, G. Tian, X. Li, Z. Yang, F. Wang, Z. Tian, B. Huang, F. Wei, K. Zha, Z. Sun, X. Sui, S. Liu, W. Guo, Q. Guo, Research Progress on Stem Cell Therapies for Articular Cartilage Regeneration, Stem Cells International 2021 (2021) 8882505.

[21] E.A. Makris, A.H. Gomoll, K.N. Malizos, J.C. Hu, K.A. Athanasiou, Repair and tissue engineering techniques for articular cartilage, Nat Rev Rheumatol 11(1) (2015) 21-34.
[22] L. Wang, M. Lazebnik, M.S. Detamore, Hyaline cartilage cells outperform mandibular condylar cartilage cells in a TMJ fibrocartilage tissue engineering application, Osteoarthritis and Cartilage 17(3) (2009) 346-353.
[23] A. Gobbi, P. Nunag, K. Malinowski, Treatment of full thickness chondral lesions of the knee with microfracture in a group of athletes, Knee Surgery, Sports Traumatology, Arthroscopy 13(3) (2005) 213-221.
[24] D. Van Assche, F. Staes, D. Van Caspel, J. Vanlauwe, J. Bellemans, D.B. Saris, F.P. Luyten, Autologous chondrocyte implantation versus microfracture for knee cartilage injury: a prospective randomized trial, with 2-year follow-up, Knee Surgery, Sports Traumatology, Arthroscopy 18(4) (2010) 486-495.
[25] M. Volz, J. Schaumburger, H. Frick, J. Grifka, S. Anders, A randomized controlled trial demonstrating sustained benefit of Autologous Matrix-Induced Chondrogenesis over microfracture at five years, International Orthopaedics 41(4) (2017) 797-804.
[26] P.C. Kreuz, M.R. Steinwachs, C. Erggelet, S.J. Krause, G. Konrad, M. Uhl, N. Südkamp, Results after microfracture of full-thickness chondral defects in different compartments in the knee, Osteoarthritis and Cartilage 14(11) (2006) 1119-1125.
[27] Y. Nakagawa, T. Suzuki, H. Kuroki, M. Kobayashi, Y. Okamoto, T. Nakamura, The effect of surface incongruity of grafted plugs in osteochondral grafting: a report of five cases, Knee Surgery, Sports Traumatology, Arthroscopy 15(5) (2007) 591-596.
[28] C. Carulli, F. Matassi, S. Soderi, L. Nistri, R. Civinini, M. Innocenti, Open Traumatic Osteochondral Fracture of the Femoral Medial Condyle and Trochlea Treated by Mosaicplasty: A Case Report at 11-Year Follow-Up, HSS Journal® 10(3) (2014) 276-279.
[29] P.C. Kreuz, M. Steinwachs, C. Erggelet, A. Lahm, P. Henle, P. Niemeyer, Mosaicplasty with Autogenous Talar Autograft for Osteochondral Lesions of the Talus after Failed Primary Arthroscopic Management: A Prospective Study with a 4-Year Follow-up, The American Journal of Sports Medicine 34(1) (2006) 55-63.
[30] A. Kar, N.D. Demirkıran, H. Tatari, B. Uzun, F. Ertem, Hexagonal grafts in mosaicplasty: Biomechanical comparison of standard cylindrical and novel hexagonal grafts in calf cadaver model, Acta Orthopaedica et Traumatologica Turcica 51(2) (2017) 160-164.
[31] J.D.F. Calder, M.S. Ballal, R.S. Deol, C.J. Pearce, P. Hamilton, M. Lutz, Histological evaluation of calcaneal tuberosity cartilage – A proposed donor site for osteochondral autologous transplant for talar dome osteochondral lesions, Foot and Ankle Surgery 21(3) (2015) 193-197.
[32] R.P. Jakob, T. Franz, E. Gautier, P. Mainil-Varlet, Autologous Osteochondral Grafting in the Knee: Indication, Results, and Reflections, Clinical Orthopaedics and Related Research (1976-2007) 401 (2002).
[33] S.D. Cook, S.L. Salkeld, L.P. Patron, E.S. Doughty, D.G. Jones, The Effect of Low-Intensity Pulsed Ultrasound on Autologous Osteochondral Plugs in a Canine Model, The American Journal of Sports Medicine 36(9) (2008) 1733-1741.
[34] D. Wang, B. Chang, F.R. Coxe, M.D. Pais, T.L. Wickiewicz, R.F. Warren, S.A. Rodeo, R.J. Williams, Clinically Meaningful Improvement After Treatment of Cartilage Defects of the Knee With Osteochondral Grafts, The American Journal of Sports Medicine 47(1) (2018) 71-81.
[35] D. Wang, N. Marom, F.R. Coxe, V. Kalia, A.J. Burge, K.J. Jones, S.A. Rodeo, R.J. Williams, Preoperative Grades of Osteoarthritis and Meniscus Volume Correlate with Clinical Outcomes of Osteochondral Graft Treatment for Cartilage Defects in the Knee, CARTILAGE 12(3) (2019) 344-353.
[36] G. E., K. D., J.R. P., Treatment of cartilage defects of the talus by autologous osteochondral grafts, The Journal of Bone and Joint Surgery. British volume 84-B(2) (2002) 237-244.
[37] G. Knutsen, J.O. Drogset, L. Engebretsen, T. Grøntvedt, V. Isaksen, T.C. Ludvigsen, S. Roberts, E. Solheim, T. Strand, O. Johansen, A Randomized Trial Comparing Autologous Chondrocyte Implantation with Microfracture: Findings at Five Years, JBJS 89(10) (2007).
[38] M.K. Demange, T. Minas, A. von Keudell, S. Sodha, T. Bryant, A.H. Gomoll, Intralesional Osteophyte Regrowth Following Autologous Chondrocyte Implantation after Previous Treatment with Marrow Stimulation Technique, CARTILAGE 8(2) (2016) 131-138.
[39] S. Vedicherla, C.T. Buckley, Cell-based therapies for intervertebral disc and cartilage regeneration-Current concepts, parallels, and perspectives, J Orthop Res 35(1) (2017) 8-22.
[40] J.J. Wood, M.A. Malek, F.J. Frassica, J.A. Polder, A.K. Mohan, E.T. Bloom, M.M. Braun, T.R. Coté, Autologous Cultured Chondrocytes: Adverse Events Reported to the United States Food and Drug Administration, JBJS 88(3) (2006).
[41] Tissue Engineering: An Alternative to Repair Cartilage, Tissue Engineering Part B: Reviews 25(4) (2019) 357-373.
[42] J.S. Temenoff, A.G. Mikos, Review: tissue engineering for regeneration of articular cartilage,

Biomaterials 21(5) (2000) 431-440.
[43] O. Haddo, S. Mahroof, D. Higgs, L. David, J. Pringle, M. Bayliss, S.R. Cannon, T.W.R. Briggs, The use of chondrogide membrane in autologous chondrocyte implantation, The Knee 11(1) (2004) 51-55.
[44] Y. Xiang, V. Bunpetch, W. Zhou, H. Ouyang, Optimization strategies for ACI: A step-chronicle review, Journal of Orthopaedic Translation 17 (2019) 3-14.
[45] H. Nejadnik, J.H. Hui, E.P. Feng Choong, B.-C. Tai, E.H. Lee, Autologous Bone Marrow–Derived Mesenchymal Stem Cells Versus Autologous Chondrocyte Implantation: An Observational Cohort Study, The American Journal of Sports Medicine 38(6) (2010) 1110-1116.
[46] M. Itokazu, S. Wakitani, H. Mera, Y. Tamamura, Y. Sato, M. Takagi, H. Nakamura, Transplantation of Scaffold-Free Cartilage-Like Cell-Sheets Made from Human Bone Marrow Mesenchymal Stem Cells for Cartilage Repair: A Preclinical Study, CARTILAGE 7(4) (2016) 361-372.
[47] K.J. Jones, B.M. Cash, Matrix-Induced Autologous Chondrocyte Implantation With Autologous Bone Grafting for Osteochondral Lesions of the Femoral Trochlea, Arthroscopy Techniques 8(3) (2019) e259-e266.
[48] M. Bhattacharjee, J. Coburn, M. Centola, S. Murab, A. Barbero, D.L. Kaplan, I. Martin, S. Ghosh, Tissue engineering strategies to study cartilage development, degeneration and regeneration, Adv Drug Deliv Rev 84 (2015) 107-22.
[49] G. Chen, T. Sato, T. Ushida, N. Ochiai, T. Tateishi, Tissue engineering of cartilage using a hybrid scaffold of synthetic polymer and collagen, Tissue engineering 10(3-4) (2004) 323-330.
[50] Y. Zhang, J. Yu, K. Ren, J. Zuo, J. Ding, X. Chen, Thermosensitive Hydrogels as Scaffolds for Cartilage Tissue Engineering, Biomacromolecules 20(4) (2019) 1478-1492.
[51] A.J. Roelofs, J.P. Rocke, C. De Bari, Cell-based approaches to joint surface repair: a research perspective, Osteoarthritis Cartilage 21(7) (2013) 892-900.
[52] K. Stuckensen, A. Schwab, M. Knauer, E. Muinos-Lopez, F. Ehlicke, J. Reboredo, F. Granero-Molto, U. Gbureck, F. Prosper, H. Walles, J. Groll, Tissue Mimicry in Morphology and Composition Promotes Hierarchical Matrix Remodeling of Invading Stem Cells in Osteochondral and Meniscus Scaffolds, Adv Mater 30(28) (2018) e1706754.
[53] T. Nagai, K.S. Furukawa, M. Sato, T. Ushida, J. Mochida, Characteristics of a Scaffold-Free Articular Chondrocyte Plate Grown in Rotational Culture, Tissue Engineering Part A 14(7) (2008) 1183-1193.
[54] A.M. Yousefi, M.E. Hoque, R.G. Prasad, N. Uth, Current strategies in multiphasic scaffold design for osteochondral tissue engineering: A review, J Biomed Mater Res A 103(7) (2015) 2460-81.
[55] M. Sittinger, D.W. Hutmacher, M.V. Risbud, Current strategies for cell delivery in cartilage and bone regeneration, Current Opinion in Biotechnology 15(5) (2004) 411-8.
[56] B.N. Mason, A. Starchenko, R.M. Williams, L.J. Bonassar, C.A. Reinhart-King, Tuning three-dimensional collagen matrix stiffness independently of collagen concentration modulates endothelial cell behavior, Acta Biomaterialia 9(1) (2013) 4635-44.
[57] Q.L. Loh, C. Choong, Three-dimensional scaffolds for tissue engineering applications: role of porosity and pore size, Tissue Eng Part B Rev 19(6) (2013) 485-502.
[58] K.S. Ogueri, T. Jafari, J.L. Escobar Ivirico, C.T. Laurencin, Polymeric Biomaterials for Scaffold-Based Bone Regenerative Engineering, Regenerative Engineering and Translational Medicine 5(2) (2019) 128-154.
[59] B. Demirbag, P.Y. Huri, G.T. Kose, A. Buyuksungur, V. Hasirci, Advanced cell therapies with and without scaffolds, Biotechnology Journal 6(12) (2011) 1437-1453.
[60] W.J. Li, R. Tuli, C. Okafor, A. Derfoul, K.G. Danielson, D.J. Hall, R.S. Tuan, A three-dimensional nanofibrous scaffold for cartilage tissue engineering using human mesenchymal stem cells, Biomaterials 26(6) (2005) 599-609.
[61] M.M. Caron, P.J. Emans, M.M. Coolsen, L. Voss, D.A. Surtel, A. Cremers, L.W. van Rhijn, T.J. Welting, Redifferentiation of dedifferentiated human articular chondrocytes: comparison of 2D and 3D cultures, Osteoarthritis Cartilage 20(10) (2012) 1170-8.
[62] Z. Yang, T. Zhao, C. Gao, F. Cao, H. Li, Z. Liao, L. Fu, P. Li, W. Chen, Z. Sun, S. Jiang, Z. Tian, G. Tian, K. Zha, T. Pan, X. Li, X. Sui, Z. Yuan, S. Liu, Q. Guo, 3D-Bioprinted Difunctional Scaffold for In Situ Cartilage Regeneration Based on Aptamer-Directed Cell Recruitment and Growth Factor-Enhanced Cell Chondrogenesis, ACS Appl Mater Interfaces 13(20) (2021) 23369-23383.
[63] Y. Guo, T. Yuan, Z. Xiao, P. Tang, Y. Xiao, Y. Fan, X. Zhang, Hydrogels of collagen/chondroitin sulfate/hyaluronan interpenetrating polymer network for cartilage tissue engineering, J Mater Sci Mater Med 23(9) (2012) 2267-79.
[64] B. Grigolo, G. Lisignoli, A. Piacentini, M. Fiorini, P. Gobbi, G. Mazzotti, M. Duca, A. Pavesio, A. Facchini, Evidence for redifferentiation of human chondrocytes grown on a hyaluronan-based biomaterial (HYAFF®11): molecular, immunohistochemical and ultrastructural analysis, Biomaterials 23(4) (2002) 1187-

1195.
[65] K.-S. Park, B.-J. Kim, E. Lih, W. Park, S.-H. Lee, Y.K. Joung, D.K. Han, Versatile effects of magnesium hydroxide nanoparticles in PLGA scaffold–mediated chondrogenesis, Acta Biomaterialia 73 (2018) 204-216.
[66] X. Wang, S. Xu, S. Zhou, W. Xu, M. Leary, P. Choong, M. Qian, M. Brandt, Y.M. Xie, Topological design and additive manufacturing of porous metals for bone scaffolds and orthopaedic implants: A review, Biomaterials 83 (2016) 127-41.
[67] S.J. Lee, D. Lee, T.R. Yoon, H.K. Kim, H.H. Jo, J.S. Park, J.H. Lee, W.D. Kim, I.K. Kwon, S.A. Park, Surface modification of 3D-printed porous scaffolds via mussel-inspired polydopamine and effective immobilization of rhBMP-2 to promote osteogenic differentiation for bone tissue engineering, Acta Biomaterialia 40 (2016) 182-191.
[68] H. Madry, A. Rey-Rico, J.K. Venkatesan, B. Johnstone, M. Cucchiarini, Transforming Growth Factor Beta-Releasing Scaffolds for Cartilage Tissue Engineering, Tissue Engineering Part B: Reviews 20(2) (2013) 106-125.
[69] N.C. Negrini, M. Bonnetier, G. Giatsidis, D.P. Orgill, S. Farè, B. Marelli, Tissue-mimicking gelatin scaffolds by alginate sacrificial templates for adipose tissue engineering, Acta Biomaterialia 87 (2019) 61-75.
[70] W. Shi, M. Sun, X. Hu, B. Ren, J. Cheng, C. Li, X. Duan, X. Fu, J. Zhang, H. Chen, Y. Ao, Structurally and Functionally Optimized Silk-Fibroin-Gelatin Scaffold Using 3D Printing to Repair Cartilage Injury In Vitro and In Vivo, Adv Mater 29(29) (2017).
[71] R. Chaudhuri, M. Ramachandran, P. Moharil, M. Harumalani, A.K. Jaiswal, Biomaterials and cells for cardiac tissue engineering: Current choices, Mater Sci Eng C Mater Biol Appl 79 (2017) 950-957.
[72] W. Linhart, F. Peters, W. Lehmann, K. Schwarz, A.F. Schilling, M. Amling, J.M. Rueger, M. Epple, Biologically and chemically optimized composites of carbonated apatite and polyglycolide as bone substitution materials, Journal of Biomedical Materials Research 54(2) (2001) 162-171.
[73] J. Suganuma, H. Alexander, Biological response of intramedullary bone to poly-L-lactic acid, Journal of Applied Biomaterials 4(1) (1993) 13-27.
[74] K.A. Athanasiou, G.G. Niederauer, C.M. Agrawal, Sterilization, toxicity, biocompatibility and clinical applications of polylactic acid/ polyglycolic acid copolymers, Biomaterials 17(2) (1996) 93-102.
[75] L. Meinel, S. Hofmann, V. Karageorgiou, C. Kirker-Head, J. McCool, G. Gronowicz, L. Zichner, R. Langer, G. Vunjak-Novakovic, D.L. Kaplan, The inflammatory responses to silk films in vitro and in vivo, Biomaterials 26(2) (2005) 147-55.
[76] F. Liu, Q. Ran, M. Zhao, T. Zhang, D.Z. Zhang, Z. Su, Additively Manufactured Continuous Cell-Size Gradient Porous Scaffolds: Pore Characteristics, Mechanical Properties and Biological Responses In Vitro, Materials (Basel) 13(11) (2020).
[77] R.M. Boehler, J.G. Graham, L.D. Shea, Tissue engineering tools for modulation of the immune response, BioTechniques 51(4) (2011) 239-254.
[78] A. Crupi, A. Costa, A. Tarnok, S. Melzer, L. Teodori, Inflammation in tissue engineering: The Janus between engraftment and rejection, European Journal of Immunology 45(12) (2015) 3222-3236.
[79] M.J. Whitaker, R.A. Quirk, S.M. Howdle, K.M. Shakesheff, Growth factor release from tissue engineering scaffolds, Journal of Pharmacy and Pharmacology 53(11) (2001) 1427-1437.
[80] J. Venugopal, S. Low, A.T. Choon, S. Ramakrishna, Interaction of cells and nanofiber scaffolds in tissue engineering, Journal of Biomedical Materials Research Part B: Applied Biomaterials 84B(1) (2008) 34-48.
[81] Y. Yan, H. Chen, H. Zhang, C. Guo, K. Yang, K. Chen, R. Cheng, N. Qian, N. Sandler, Y.S. Zhang, H. Shen, J. Qi, W. Cui, L. Deng, Vascularized 3D printed scaffolds for promoting bone regeneration, Biomaterials 190-191 (2019) 97-110.
[82] N. Masoumi, K.L. Johnson, M.C. Howell, G.C. Engelmayr, Valvular interstitial cell seeded poly(glycerol sebacate) scaffolds: Toward a biomimetic in vitro model for heart valve tissue engineering, Acta Biomaterialia 9(4) (2013) 5974-5988.
[83] S.H. Lee, B.S. Kim, S.H. Kim, S.W. Kang, Y.H. Kim, Thermally produced biodegradable scaffolds for cartilage tissue engineering, Macromolecular Bioscience 4(8) (2004) 802-10.
[84] T. Cui, J. Yu, Q. Li, C.F. Wang, S. Chen, W. Li, G. Wang, Large-Scale Fabrication of Robust Artificial Skins from a Biodegradable Sealant-Loaded Nanofiber Scaffold to Skin Tissue via Microfluidic Blow-Spinning, Adv Mater 32(32) (2020) e2000982.
[85] Y. Li, Y. Xiao, C. Liu, The Horizon of Materiobiology: A Perspective on Material-Guided Cell Behaviors and Tissue Engineering, Chem Rev 117(5) (2017) 4376-4421.
[86] Z. Alvarez, M.A. Mateos-Timoneda, P. Hyrossova, O. Castano, J.A. Planell, J.C. Perales, E. Engel, S. Alcantara, The effect of the composition of PLA films and lactate release on glial and neuronal maturation and the maintenance of the neuronal progenitor niche, Biomaterials 34(9) (2013) 2221-33.

[87] H. Yoshimoto, Y.M. Shin, H. Terai, J.P. Vacanti, A biodegradable nanofiber scaffold by electrospinning and its potential for bone tissue engineering, Biomaterials 24(12) (2003) 2077-2082.
[88] C.R. Kothapalli, M.T. Shaw, M. Wei, Biodegradable HA-PLA 3-D porous scaffolds: effect of nano-sized filler content on scaffold properties, Acta Biomaterialia 1(6) (2005) 653-62.
[89] K. Rezwan, Q.Z. Chen, J.J. Blaker, A.R. Boccaccini, Biodegradable and bioactive porous polymer/inorganic composite scaffolds for bone tissue engineering, Biomaterials 27(18) (2006) 3413-31.
[90] H.-Y. Cheung, K.-T. Lau, T.-P. Lu, D. Hui, A critical review on polymer-based bio-engineered materials for scaffold development, Composites Part B: Engineering 38(3) (2007) 291-300.
[91] S. Agarwal, J.H. Wendorff, A. Greiner, Progress in the Field of Electrospinning for Tissue Engineering Applications, Advanced Materials 21(32-33) (2009) 3343-3351.
[92] S.J. Bryant, F.J. Vernerey, Programmable Hydrogels for Cell Encapsulation and Neo-Tissue Growth to Enable Personalized Tissue Engineering, Advanced healthcare materials 7(1) (2018) 1700605.
[93] S. Lin, L.A. Hapach, C. Reinhart-King, L. Gu, Towards Tuning the Mechanical Properties of Three-Dimensional Collagen Scaffolds Using a Coupled Fiber-Matrix Model, Materials (Basel) 8(8) (2015) 5376-5384.
[94] M. Simonet, N. Stingelin, J.G.F. Wismans, C.W.J. Oomens, A. Driessen-Mol, F.P.T. Baaijens, Tailoring the void space and mechanical properties in electrospun scaffolds towards physiological ranges, J Mater Chem B 2(3) (2014) 305-313.
[95] M. Achilli, D. Mantovani, Tailoring Mechanical Properties of Collagen-Based Scaffolds for Vascular Tissue Engineering: The Effects of pH, Temperature and Ionic Strength on Gelation, Polymers 2(4) (2010) 664-680.
[96] M. Farokhi, F. Mottaghitalab, Y. Fatahi, M.R. Saeb, P. Zarrintaj, S.C. Kundu, A. Khademhosseini, Silk fibroin scaffolds for common cartilage injuries: Possibilities for future clinical applications, European Polymer Journal 115 (2019) 251-267.
[97] H. Janik, M. Marzec, A review: fabrication of porous polyurethane scaffolds, Mater Sci Eng C Mater Biol Appl 48 (2015) 586-91.
[98] M.J. Dewey, D.J. Milner, D. Weisgerber, C.L. Flanagan, M. Rubessa, S. Lotti, K.M. Polkoff, S. Crotts, S.J. Hollister, M.B. Wheeler, B.A.C. Harley, Repair of critical-size porcine craniofacial bone defects using a collagen-polycaprolactone composite biomaterial, bioRxiv (2021) 2021.04.19.440506.
[99] L. Nimeskern, G.J.V.M. van Osch, R. Müller, K.S. Stok, Quantitative Evaluation of Mechanical Properties in Tissue-Engineered Auricular Cartilage, Tissue Engineering Part B: Reviews 20(1) (2013) 17-27.
[100] K.H. Chang, H.T. Liao, J.P. Chen, Preparation and characterization of gelatin/hyaluronic acid cryogels for adipose tissue engineering: in vitro and in vivo studies, Acta Biomaterialia 9(11) (2013) 9012-26.
[101] H. Montazerian, M.G.A. Mohamed, M.M. Montazeri, S. Kheiri, A.S. Milani, K. Kim, M. Hoorfar, Permeability and mechanical properties of gradient porous PDMS scaffolds fabricated by 3D-printed sacrificial templates designed with minimal surfaces, Acta Biomaterialia 96 (2019) 149-160.
[102] R. Ikeda, H. Fujioka, I. Nagura, T. Kokubu, N. Toyokawa, A. Inui, T. Makino, H. Kaneko, M. Doita, M. Kurosaka, The effect of porosity and mechanical property of a synthetic polymer scaffold on repair of osteochondral defects, Int Orthop 33(3) (2009) 821-8.
[103] S. Arabnejad, R. Burnett Johnston, J.A. Pura, B. Singh, M. Tanzer, D. Pasini, High-strength porous biomaterials for bone replacement: A strategy to assess the interplay between cell morphology, mechanical properties, bone ingrowth and manufacturing constraints, Acta Biomaterialia 30 (2016) 345-356.
[104] A. Bandyopadhyay, F. Espana, V.K. Balla, S. Bose, Y. Ohgami, N.M. Davies, Influence of porosity on mechanical properties and in vivo response of Ti6Al4V implants, Acta Biomaterialia 6(4) (2010) 1640-1648.
[105] Q. Fu, E. Saiz, M.N. Rahaman, A.P. Tomsia, Bioactive glass scaffolds for bone tissue engineering: state of the art and future perspectives, Materials Science and Engineering: C 31(7) (2011) 1245-1256.
[106] H.-Y. Lee, J.-E. Won, U.S. Shin, H.-W. Kim, Using hydrophilic ionic liquids as a facile route to prepare porous-structured biopolymer scaffolds, Materials Letters 65(14) (2011) 2114-2117.
[107] Y. Jing, L. Zhang, R. Huang, D. Bai, H. Bai, Q. Zhang, Q. Fu, Ultrahigh-performance electrospun polylactide membranes with excellent oil/water separation ability via interfacial stereocomplex crystallization, Journal of Materials Chemistry A 5(37) (2017) 19729-19737.
[108] J. Yang, Y. Li, Y. Liu, D. Li, L. Zhang, Q. Wang, Y. Xiao, X. Zhang, Influence of hydrogel network microstructures on mesenchymal stem cell chondrogenesis in vitro and in vivo, Acta Biomaterialia 91 (2019) 159-172.
[109] H. Zhao, L. Li, S. Ding, C. Liu, J. Ai, Effect of porous structure and pore size on mechanical strength of 3D-printed comby scaffolds, Materials Letters 223 (2018) 21-24.
[110] H.M. Aydin, A.J. El Haj, E. Piskin, Y. Yang, Improving pore interconnectivity in polymeric scaffolds

for tissue engineering, Journal of Tissue Engineering and Regenerative Medicine 3(6) (2009) 470-6.
[111] A.C. Jones, C.H. Arns, D.W. Hutmacher, B.K. Milthorpe, A.P. Sheppard, M.A. Knackstedt, The correlation of pore morphology, interconnectivity and physical properties of 3D ceramic scaffolds with bone ingrowth, Biomaterials 30(7) (2009) 1440-1451.
[112] B.B. Mandal, S.C. Kundu, Cell proliferation and migration in silk fibroin 3D scaffolds, Biomaterials 30(15) (2009) 2956-65.
[113] R.C. Atwood, J.R. Jones, P.D. Lee, L.L. Hench, Analysis of pore interconnectivity in bioactive glass foams using X-ray microtomography, Scripta Materialia 51(11) (2004) 1029-1033.
[114] Q. Liu, J. Wang, Y. Chen, Z. Zhang, L. Saunders, E. Schipani, Q. Chen, P.X. Ma, Suppressing mesenchymal stem cell hypertrophy and endochondral ossification in 3D cartilage regeneration with nanofibrous poly(l-lactic acid) scaffold and matrilin-3, Acta Biomaterialia 76 (2018) 29-38.
[115] S.I. Somo, B. Akar, E.S. Bayrak, J.C. Larson, A.A. Appel, H. Mehdizadeh, A. Cinar, E.M. Brey, Pore Interconnectivity Influences Growth Factor-Mediated Vascularization in Sphere-Templated Hydrogels, Tissue Eng Part C Methods 21(8) (2015) 773-85.
[116] Y. Xie, K. Lee, X. Wang, T. Yoshitomi, N. Kawazoe, Y. Yang, G. Chen, Interconnected collagen porous scaffolds prepared with sacrificial PLGA sponge templates for cartilage tissue engineering, Journal of Materials Chemistry B 9(40) (2021) 8491-8500.
[117] W. Sun, D.M. Tiemessen, M. Sloff, R.J. Lammers, E.L. de Mulder, J. Hilborn, B. Gupta, W.F. Feitz, W.F. Daamen, T.H. van Kuppevelt, P.J. Geutjes, E. Oosterwijk, Improving the cell distribution in collagen-coated poly-caprolactone knittings, Tissue Eng Part C Methods 18(10) (2012) 731-9.
[118] F.P. Melchels, A.M. Barradas, C.A. van Blitterswijk, J. de Boer, J. Feijen, D.W. Grijpma, Effects of the architecture of tissue engineering scaffolds on cell seeding and culturing, Acta Biomaterialia 6(11) (2010) 4208-17.
[119] H. Tsuji, T. Tsuruno, Water Vapor Permeability of Poly(L-lactide)/Poly(D-lactide) Stereocomplexes, Macromolecular Materials and Engineering 295(8) (2010) 709-715.
[120] B. Pasha Mahammod, E. Barua, A.B. Deoghare, K.M. Pandey, Permeability quantification of porous polymer scaffold for bone tissue engineering, Materials Today: Proceedings 22 (2020) 1687-1693.
[121] Y. Reinwald, R.K. Johal, A.M. Ghaemmaghami, F.R.A.J. Rose, S.M. Howdle, K.M. Shakesheff, Interconnectivity and permeability of supercritical fluid-foamed scaffolds and the effect of their structural properties on cell distribution, Polymer 55(1) (2014) 435-444.
[122] J.M. Kemppainen, S.J. Hollister, Differential effects of designed scaffold permeability on chondrogenesis by chondrocytes and bone marrow stromal cells, Biomaterials 31(2) (2010) 279-287.
[123] Q. Zhang, H. Lu, N. Kawazoe, G. Chen, Pore size effect of collagen scaffolds on cartilage regeneration, Acta Biomaterialia 10(5) (2014) 2005-2013.
[124] M.J. Gupte, W.B. Swanson, J. Hu, X. Jin, H. Ma, Z. Zhang, Z. Liu, K. Feng, G. Feng, G. Xiao, N. Hatch, Y. Mishina, P.X. Ma, Pore size directs bone marrow stromal cell fate and tissue regeneration in nanofibrous macroporous scaffolds by mediating vascularization, Acta Biomaterialia 82 (2018) 1-11.
[125] X. Feng, P. Xu, T. Shen, Y. Zhang, J. Ye, C. Gao, Influence of pore architectures of silk fibroin/collagen composite scaffolds on the regeneration of osteochondral defects in vivo, Journal of Materials Chemistry B 8(3) (2020) 391-405.
[126] S. Chen, Q. Zhang, T. Nakamoto, N. Kawazoe, G. Chen, Gelatin Scaffolds with Controlled Pore Structure and Mechanical Property for Cartilage Tissue Engineering, Tissue Engineering Part C: Methods 22(3) (2015) 189-198.
[127] S.-M. Lien, L.-Y. Ko, T.-J. Huang, Effect of pore size on ECM secretion and cell growth in gelatin scaffold for articular cartilage tissue engineering, Acta Biomaterialia 5(2) (2009) 670-679.
[128] F.J. O'Brien, B.A. Harley, I.V. Yannas, L.J. Gibson, The effect of pore size on cell adhesion in collagen-GAG scaffolds, Biomaterials 26(4) (2005) 433-41.
[129] S.H. Oh, T.H. Kim, G.I. Im, J.H. Lee, Investigation of Pore Size Effect on Chondrogenic Differentiation of Adipose Stem Cells Using a Pore Size Gradient Scaffold, Biomacromolecules 11(8) (2010) 1948-1955.
[130] C. Liu, Z. Xia, J.T. Czernuszka, Design and Development of Three-Dimensional Scaffolds for Tissue Engineering, Chemical Engineering Research and Design 85(7) (2007) 1051-1064.
[131] M.J. Moore, E. Jabbari, E.L. Ritman, L. Lu, B.L. Currier, A.J. Windebank, M.J. Yaszemski, Quantitative analysis of interconnectivity of porous biodegradable scaffolds with micro-computed tomography, J Biomed Mater Res A 71(2) (2004) 258-67.
[132] S. Oh, Fabrication and characterization of hydrophilic poly(lactic-co-glycolic acid)/poly(vinyl alcohol) blend cell scaffolds by melt-molding particulate-leaching method, Biomaterials 24(22) (2003) 4011-4021.
[133] L. Liu, Y. Wang, S. Guo, Z. Wang, W. Wang, Porous polycaprolactone/nanohydroxyapatite tissue

engineering scaffolds fabricated by combining NaCl and PEG as co-porogens: structure, property, and chondrocyte-scaffold interaction in vitro, J Biomed Mater Res B Appl Biomater 100(4) (2012) 956-66.
[134] D. Sin, X. Miao, G. Liu, F. Wei, G. Chadwick, C. Yan, T. Friis, Polyurethane (PU) scaffolds prepared by solvent casting/particulate leaching (SCPL) combined with centrifugation, Materials Science and Engineering: C 30(1) (2010) 78-85.
[135] Q. Zhou, Y. Gong, C. Gao, Microstructure and mechanical properties of poly(L-lactide) scaffolds fabricated by gelatin particle leaching method, Journal of Applied Polymer Science 98(3) (2005) 1373-1379.
[136] L. Liu, X. Wang, J. Zhou, H. Chu, D. Shen, H. Chen, S. Qin, Investigation of pore structure and mechanical property of cement paste subjected to the coupled action of freezing/thawing and calcium leaching, Cement and Concrete Research 109 (2018) 133-146.
[137] L. Leung, C. Chan, S. Baek, H. Naguib, Comparison of morphology and mechanical properties of PLGA bioscaffolds, Biomedical Materials (Bristol, England) 3(2) (2008) 025006.
[138] H. Janik, M. Marzec, A review: Fabrication of porous polyurethane scaffolds, Materials Science and Engineering: C 48 (2015) 586-591.
[139] D. Boland Eugene, A. Telemeco Todd, G. Simpson David, E. Wnek Gary, L. Bowlin Gary, Utilizing acid pretreatment and electrospinning to improve biocompatibility of poly(glycolic acid) for tissue engineering, Journal of Biomedical Materials Research Part B: Applied Biomaterials 71B(1) (2004) 144-152.
[140] S. Gautam, C.F. Chou, A.K. Dinda, P.D. Potdar, N.C. Mishra, Surface modification of nanofibrous polycaprolactone/gelatin composite scaffold by collagen type I grafting for skin tissue engineering, Mater Sci Eng C Mater Biol Appl 34 (2014) 402-9.
[141] M. Mabrouk, H.H. Beherei, D.B. Das, Recent progress in the fabrication techniques of 3D scaffolds for tissue engineering, Mater Sci Eng C Mater Biol Appl 110 (2020) 110716.
[142] Y. He, M. Tian, X. Li, J. Hou, S. Chen, G. Yang, X. Liu, S. Zhou, A Hierarchical-Structured Mineralized Nanofiber Scaffold with Osteoimmunomodulatory and Osteoinductive Functions for Enhanced Alveolar Bone Regeneration, Advanced healthcare materials n/a(n/a) 2102236.
[143] X. Zong, H. Bien, C.Y. Chung, L. Yin, D. Fang, B.S. Hsiao, B. Chu, E. Entcheva, Electrospun fine-textured scaffolds for heart tissue constructs, Biomaterials 26(26) (2005) 5330-8.
[144] N. Bhardwaj, S.C. Kundu, Electrospinning: a fascinating fiber fabrication technique, Biotechnology Advances 28(3) (2010) 325-47.
[145] B. Dong, O. Arnoult, M.E. Smith, G.E. Wnek, Electrospinning of collagen nanofiber scaffolds from benign solvents, Macromol Rapid Commun 30(7) (2009) 539-42.
[146] A. Haider, S. Haider, I.-K. Kang, A comprehensive review summarizing the effect of electrospinning parameters and potential applications of nanofibers in biomedical and biotechnology, Arabian Journal of Chemistry 11(8) (2018) 1165-1188.
[147] L. Wang, R.E. Lee, G. Wang, R.K.M. Chu, J. Zhao, C.B. Park, Use of stereocomplex crystallites for fully-biobased microcellular low-density poly(lactic acid) foams for green packaging, Chemical Engineering Journal 327 (2017) 1151-1162.
[148] J.-N. Huang, X. Jing, L.-H. Geng, B.-Y. Chen, H.-Y. Mi, X.-F. Peng, A novel multiple soaking temperature (MST) method to prepare polylactic acid foams with bi-modal open-pore structure and their potential in tissue engineering applications, The Journal of Supercritical Fluids 103 (2015) 28-37.
[149] L. Lu, S.J. Peter, M. D. Lyman, H.-L. Lai, S.M. Leite, J.A. Tamada, S. Uyama, J.P. Vacanti, L. Robert, A.G. Mikos, In vitro and in vivo degradation of porous poly(dl-lactic-co-glycolic acid) foams, Biomaterials 21(18) (2000) 1837-1845.
[150] K.Y. Chung, N.C. Mishra, C.C. Wang, F.H. Lin, K.H. Lin, Fabricating scaffolds by microfluidics, Biomicrofluidics 3(2) (2009) 22403.
[151] Y. Liu, T. Nelson, B. Cromeens, T. Rager, J. Lannutti, J. Johnson, G.E. Besner, HB-EGF embedded in PGA/PLLA scaffolds via subcritical CO2 augments the production of tissue engineered intestine, Biomaterials 103 (2016) 150-9.
[152] A. Palmroth, S. Pitkanen, M. Hannula, K. Paakinaho, J. Hyttinen, S. Miettinen, M. Kellomaki, Evaluation of scaffold microstructure and comparison of cell seeding methods using micro-computed tomography-based tools, Journal of the Royal Society Interface 17(165) (2020) 20200102.
[153] L.M. Mathieu, M.O. Montjovent, P.E. Bourban, D.P. Pioletti, J.A. Manson, Bioresorbable composites prepared by supercritical fluid foaming, J Biomed Mater Res A 75(1) (2005) 89-97.
[154] M. Mabrouk, H.H. Beherei, D.B. Das, Recent progress in the fabrication techniques of 3D scaffolds for tissue engineering, Materials Science and Engineering: C 110 (2020) 110716.
[155] A. Eltom, G. Zhong, A. Muhammad, Scaffold Techniques and Designs in Tissue Engineering Functions and Purposes: A Review, Advances in Materials Science and Engineering 2019 (2019) 1-13.

Chapter 2

Preparation of porous collagen scaffolds using sacrificial PLGA sponge templates

2.1 Abstract

Interconnected pore structures of scaffolds are essential to control cell functions for cartilage tissue engineering. However, it has been difficult to precisely control the interconnectivity of scaffolds. In this part, collagen scaffolds with interconnected pore structures were prepared using poly($_{D,L}$-lactide-*co*-glycolide) (PLGA) sponges as sacrificial templates. The PLGA sponge templates were fabricated by a solvent casting/particulate leaching method. PLGA/NaCl weight ratio at 10:90 and 5:95 and the size of salt particulates in the ranges of 150-250, 250-355 and 355-500 μm were used to control the porosity and pore size of the PLGA sponges. And then the PLGA sponges were hybridized with collagen to form the PLGA-collagen composite constructs. After selective removal of the PLGA sponge templates from the PLGA-collagen composite constrcuts, porous collagen scaffolds were prepared. The negative replica spaces of PLGA templates formed interconnecting channels in the collagen scaffolds. The interconnecting channels in the collagen scaffolds were large when the PLGA templates prepared with 10 wt.% PLGA and large salt particulates were used. The Young's moduli of the PLGA-templated collagen scaffolds were higher than that of the control collagen scaffold in both dry and hydrated states. The Young's moduli of the collagen scaffolds increased with increasing the porosity and pore size of the sacrificial PLGA sponge templates.

2.2 Introduction

Interconnected pore structures of scaffolds are required for cell penetration and immigration [1, 2]. A variety of methods have been developed to prepare porous scaffolds [3-5]. Conventional methods such as solvent casting/particulate leaching, gas foaming, phase separation, freeze-drying and electrospinning can easily generate pore structures [6]. By these methods, however, it is difficult to precisely control pore structures, in particular, the interconnectivity of scaffolds. In recent years, some new methods have been developed to precisely control pore structures with high interconnectivity. For example, three-dimensional printing has been combined with directional freezing to control the scaffold micro- and macro-architectures [7]. Particulate leaching and electrospinning have been combined to introduce large pores in electrospun scaffolds [8, 9]. Particulate leaching and freeze-drying have been combined to introduce large pores and increase pore interconnectivity in pore scaffolds [10]. This technique uses pre-prepared ice particulates as porogen materials to create large pores with good interconnectivity [11]. Unidirectional freeze-drying has been developed to prepare unidirectional pore structures to facilitate cell seeding and tissue regeneration [12, 13].Cubic close-

packed (*ccp*) lattices of monodispersed polymer microspheres have been used as sacrificial templates to prepare inverse opal scaffolds with well-defined pore structures and good interconnection [14, 15]. In this method, the pore structures are inherited from the *ccp* lattices of microbeads. Necking between adjacent microspheres by thermal annealing, mechanical compression or chemical fusion can control the interconnectivity of inverse opal scaffolds. Microfluidics has been used to generate air bubbles or liquid droplets with defined sizes and distributions that serve as templates to precisely control the pore structures of scaffolds [16-18]. Among these methods, the ice particulate method, *ccp* method and microfluidics can precisely control pore structures. However, some defects in the packing of sacrificial particulates, microbeads and bubbles may result in local deficiency of the pore structures. To solve this problem, templates with an integral and continuous templating structure and easy fabrication are desirable.

In this part, PLGA sponges were used as sacrificial templates to precisely control the interconnectivity of collagen scaffolds. The PLGA sponges had an integral and continuous templating structure and could be easily prepared by the solvent casting/particulate leaching method. PLGA sponges with different porosities and pore sizes were used to prepare collagen scaffolds with different interconnected pore structures. An interconnected network was formed throughout the collagen scaffolds after leaching of the PLGA templates.

2.3 Materials and methods

2.3.1 Preparation of PLGA templates

Poly($_{D,L}$-lactide-*co*-glycolide) (PLGA, Sigma-Aldrich, St. Louis, MO, USA) templates were prepared by a solvent casting/particulate leaching method. NaCl particulates with three different diameter ranges of 150-250, 250-355, 355-500 μm were obtained by sieving salt particulates with sieves having the respective mesh sizes. PLGA (1 g) was dissolved in 4.5 mL of chloroform and mixed with 9.0 g of NaCl particulates of different sizes. The PLGA/NaCl mixtures were molded in aluminum pans and the chloroform was evaporated by air-drying for 7 days. After the PLGA/NaCl constructs were detached from the aluminum pans, the NaCl particulates were removed by immersing the constructs in deionized water to obtain the PLGA templates. The PLGA templates were then freeze-dried. Another set of PLGA templates was prepared by dissolving 0.5 g of PLGA in 4.5 mL of chloroform and mixing with 9.5 g of NaCl particles of different sizes. The six types of PLGA templates prepared with different PLGA/NaCl ratios and NaCl particulate sizes of 10:90 and 150-250 μm; 5:95 and 150-250 μm; 10:90 and 250-355 μm; 5:95 and 250-355 μm; 10:90 and 355-500 μm; 5:95 and 355-500 μm were referred to as PLGA-10-150, PLGA-5-150, PLGA-10-250, PLGA-5-250, PLGA-10-355 and PLGA-5-355, respectively. The PLGA templates had a diameter of 5 cm and a thickness of 5 mm.

2.3.2 Preparation of collagen scaffolds using PLGA templates

PLGA-collagen constructs were prepared by introducing collagen sponges into the pores of the PLGA templates, followed by immersion in ammonia hydroxide solution to selectively remove the PLGA templates. To prepare the PLGA-collagen constructs, the PLGA templates were immersed in 1 wt% collagen solution (Nippon Ham, Osaka, Japan) to allow all the pores of the PLGA templates to be filled with collagen solution by repeating vacuum and ventilation 5 times. The collagen solution-impregnated PLGA templates were frozen at -80 °C for 6 hours and freeze-dried for 3 days with a

freeze-dryer (FDU-2200, Tokyo Rikakikai, Tokyo, Japan). The freeze-dried PLGA-collagen constructs were crosslinked by sequential immersion in 95 (v/v)%, 90 (v/v)% and 80 (v/v)% ethanol aqueous solutions containing 50 mM 1-ethyl-3-(3-dimethylaminopropyl) carbodiimide (EDC, Peptide Institute, Osaka, Japan) and 20 mM N-hydroxysuccinimide (NHS, FUJIFILM Wako Pure Chemical, Osaka, Japan), each for 3 hours. The PLGA-collagen constructs in each cross-linking solution were degassed under vacuum to ensure that the cross-linking agents entered all the pores of the constructs. After washing with deionized water 3 times, the cross-linked PLGA-collagen constructs were immersed in 0.1 M glycine aqueous solution for 12 hours for blocking. The PLGA-collagen constructs were immersed in 3 (wt/v)% ammonia hydroxide solution for 2 days under shaking to selectively remove the PLGA templates. The obtained collagen scaffolds were washed with deionized water 6 times and freeze-dried for 48 hours. The six types of collagen scaffolds prepared from the PLGA-10-150, PLGA-5-150, PLGA-10-250, PLGA-5-250, PLGA-10-355 and PLGA-5-355 templates were referred to as Col-10-150, Col-5-150, Col-10-250, Col-5-250, Col-10-355 and Col-5-355, respectively. Control collagen scaffolds were prepared by the same procedure without the PLGA template.

2.3.3 Characterization of scaffolds

Fourier transform infrared spectroscopy-attenuated total reflectance (FTIR-ATR) spectra of the PLGA templates, PLGA-collagen constructs and collagen scaffolds were measured using an FT-IR spectrophotometer (IR Prestige-21, Shimadzu, Kyoto, Japan) equipped with a DuraSamplIR II diamond ATR accessory in the range of 3200–600 cm^{-1} at a resolution of 4 cm^{-1} and 36 scans.

The porosity of the collagen scaffolds was measured according to Archimedes' principle by the formula porosity = $V_{pore}/V = ((W_2-W_1)/\rho/V) \times 100\%$, where V_{pore} is the volume of the pore, V is the volume of the scaffold, W_1 is the dry weight of the collagen scaffold, W_2 is the wet weight of the collagen scaffold, and ρ is the density of water [19]. Three samples were used for the measurement.

For measurement of the compression strength, the PLGA-templated collagen scaffolds and control scaffold were punched into discs with a diameter of 6 mm and thickness of 3 mm. The compressive modulus of the scaffolds was measured in both dry and hydrated states. The scaffold discs were immersed in phosphate-buffered saline (PBS) for 2 hours at room temperature before testing in a hydrated state. Then, the scaffold discs were compressed at a rate of 0.1 mm/s using a texture analyzer (TA. XTPlus, Texture Technologies, Hamilton, MA, USA). The initial linear region of the stress-strain curve was used to calculate the Young's modulus. Three samples of each group were tested for the measurement.

Cross sections of the PLGA templates, PLGA-collagen constructs and collagen scaffolds were sputter-coated with platinum and then observed with a scanning electron microscope (JSM-6400Fs, JEOL, Tokyo, Japan) at an accelerating voltage of 5 kV. The interconnectivity of collagen scaffold in SEM images was analysed using the image analysis software Image J. Thirty images were used for image analysis. The total area of interconnecting pores was divided by the total area of cross-section to obtain the interconnectivity of collagen scaffold [20].

2.4 Results

2.4.1 Morphology, porosity and interconnectivity of PLGA templates, PLGA-collagen constructs and collagen scaffolds

The PLGA sponge templates were fabricated by a solvent casting/particulate leaching method (Figure 2.1a). Different ratios of PLGA/NaCl and different sizes of NaCl particulates were used to control the porosity and pore size of the PLGA sponges. SEM observation showed the porous structures of the PLGA sponges (Figure 2.1c). The pores were the negative replicas of the NaCl particulates and their size and shape were determined by the salt particulates. Pore size increased with increasing size of the salt particulates. The pore walls became thicker when a higher PLGA ratio and larger salt particulates were used. Hybridization with collagen resulted in the formation of collagen microsponges in the pores of the PLGA sponges (Figure 2.1c). After selective removal of the PLGA sponge templates, collagen scaffolds were obtained. The size of scaffolds became a little smaller after removal of PLGA templates and the collagen scaffolds had the same white appearance as that of the control (Figure 2.1b). Removal of the PLGA templates left negative replica spaces (see the red highlighted regions in the images of Figure 2.1c) in the collagen scaffolds, which formed interconnecting channels in the scaffolds. The interconnecting channels linked the pores of the collagen microsponges, making the whole pore structures well interconnected. The interconnecting channels in the collagen scaffolds were large when the PLGA templates prepared with 10 wt.% PLGA and large salt particulates were used. The interconnectivity of collagen scaffolds templated by PLGA sponge using 10 wt.% and 5 wt.% PLGA was about 17% and 13% (Table 2.1). In contrast, the interconnectivity of control collagen scaffold was 4%. The collagen scaffold prepared with PLGA-10-355 had the largest interconnecting channels. The porosity of all the scaffolds was higher than 97% (Table 2.1). The PLGA-templated collagen scaffolds had a slightly higher porosity than the control collagen scaffold. Removal of the PLGA templates slightly increased the porosity of the scaffolds.

Table 2.1 Porosity and interconnectivity of collagen scaffolds (mean ± SD, n = 3).

Scaffolds	Col-10-150	Col-10-250	Col-10-355	Col-5-150	Col-5-250	Col-5-355	Control
Porosity (%)	98.1 ± 0.6	98.3 ± 0.9	98.5 ± 0.8	97.4 ± 0.7	98.0 ± 0.9	97.5 ± 1.4	97.1 ± 1.3
Interconnectivity (%)	17.7 ±1.5%	17.0 ±2.8%	17.5 ±2.6%	13.6 ±1.2%	13.0±1.9%	13.4 ±2.2%	4.0 ± 1.3%

2.4.2 Infrared spectra and mechanical properties of collagen scaffolds

FTIR-ATR spectra of PLGA sponges, PLGA-collagen constructs and collagen scaffolds were examined to confirm the removal of the PLGA template from the PLGA-collagen construct (Figure 2.2a,b,c,d,e). The peak at 1745 cm^{-1} corresponding to the C=O stretch of the ester group in PLGA was detected in the PLGA sponge templates and PLGA-collagen constructs but did not appear in the collagen scaffold. The results confirmed that the PLGA templates were completely removed from the PLGA-collagen constructs and that no PLGA remained in the collagen scaffolds.

The mechanical properties of the collagen scaffolds in both dry and hydrated states were measured using

a static compression test (Figure 2.2g). The Young's moduli of the PLGA-templated collagen scaffolds were higher than that of the control collagen scaffold in both dry and hydrated states. The Young's moduli of the dry collagen scaffolds were higher than those of the hydrated scaffolds. The Young's moduli of the collagen scaffolds increased with increasing porosity and pore size of the sacrificial PLGA sponge templates. The collagen scaffolds were composed of collagen microsponges that formed in the PLGA sponge templates when collagen was introduced into the templates. The structure of collagen microsponges contributed to the increase in the Young's modulus. SEM observation showed the homogenous formation of collagen microsponges in the PLGA-templated collagen scaffolds, while the control collagen scaffold had random pore structures with extremely large and small pores. When the porosity of the PLGA template was increased from 90% to 95%, more spaces were present in the 95% PLGA sponge templates and more collagen could be introduced into the pores. The interconnected pores in the Col-10 scaffolds were larger than those in the Col-5 scaffolds. These two factors should explain the higher Young's moduli of the Col-5 scaffolds.

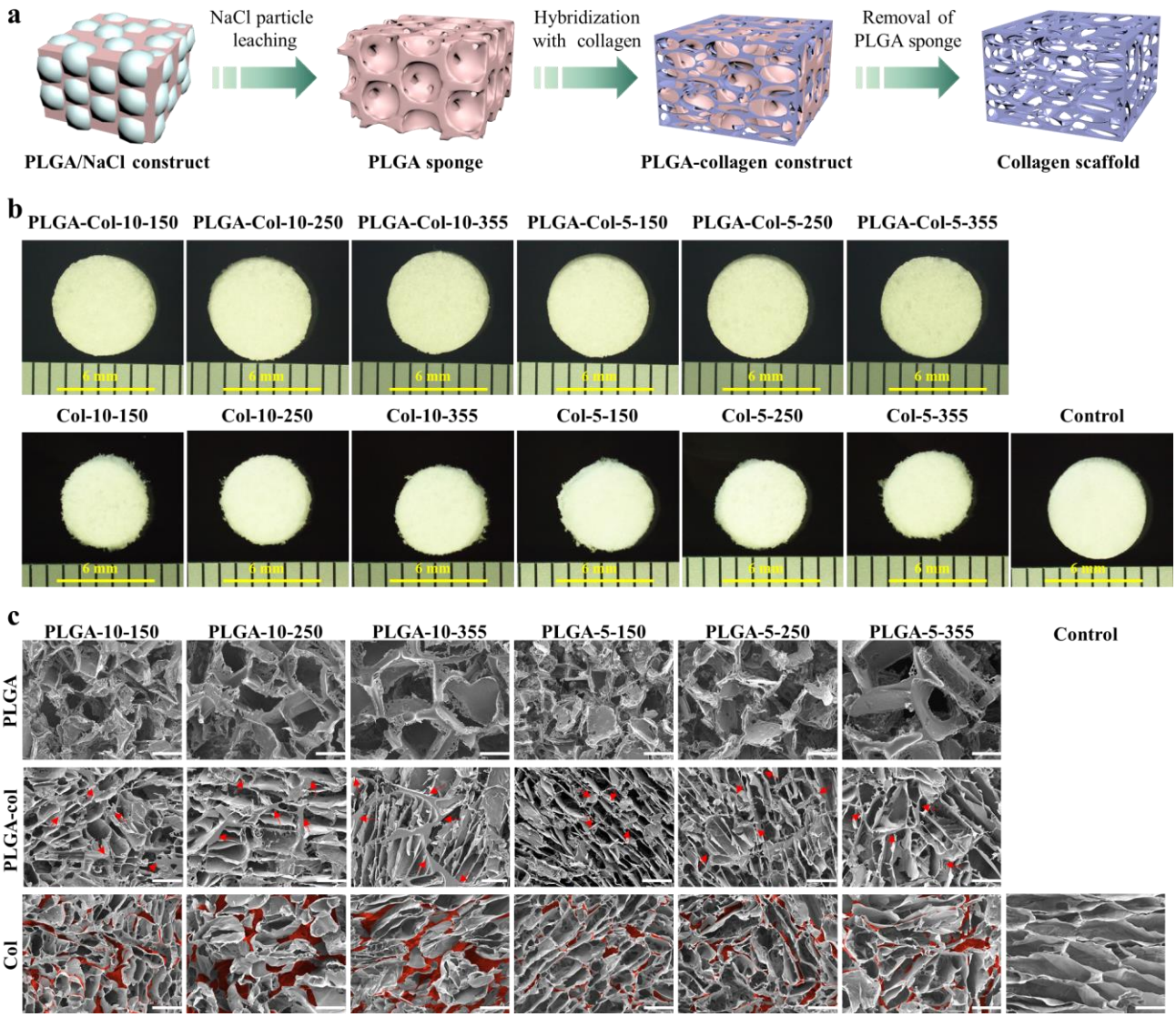

Figure 2.1 (a) Preparation scheme of interconnected collagen porous scaffolds. (b) The photomicrographs of PLGA-collagen constructs before removal of PLGA templates and the respective collagen scaffolds after removal of PLGA templates. (c) SEM images of the cross sections of PLGA templates, PLGA-collagen constructs (PLGA-col) and collagen scaffolds (Col). Red arrows indicate PLGA in the PLGA-collagen

constructs; red highlight indicates the negative replica space after the leaching of PLGA templates in the collagen scaffolds. Scale bar: 200 μm.

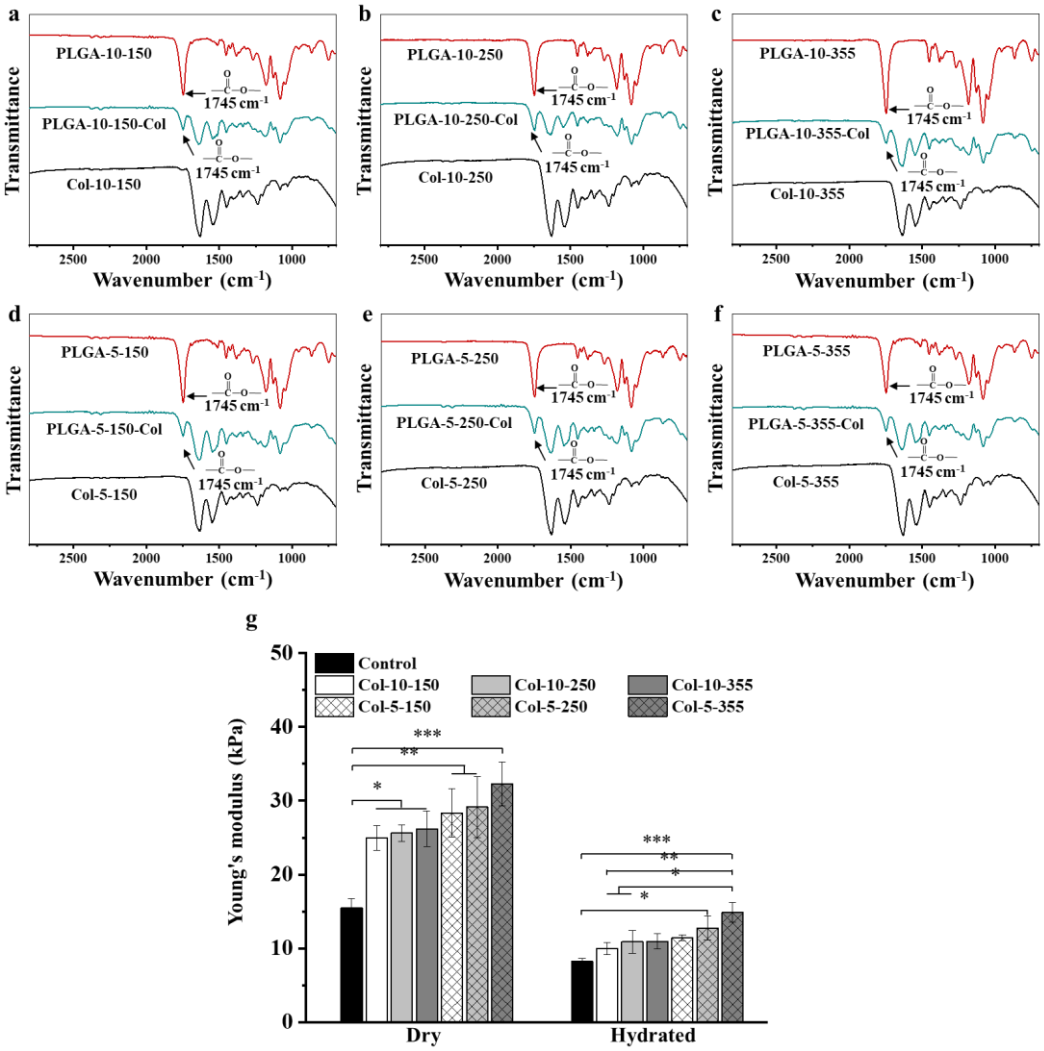

Figure 2.2 (a), (b), (c), (d), (e), (f) FTIR-ATR spectra of each PLGA templates, PLGA-collagen constructs and collagen scaffolds. (g) Compression moduli of dry and hydrated collagen scaffolds. Data represent mean ± SD, n = 3. Significant difference: *, $p < 0.05$; **, $p < 0.01$; ***, $p < 0.001$.

2.5 Discussion

In this study, interconnected collagen scaffolds were prepared for cartilage tissue engineering. The control collagen scaffold was obtained by directly freeze-drying 1 wt.% collagen solution, which had a random pore structure and poor interconnectivity. The six types of collagen scaffolds were prepared using PLGA sponges as sacrificial templates. PLGA templates with different porosities and different pore sizes were prepared by controlling the PLGA/NaCl weight ratio at 10:90 and 5:95 and the size of salt particulates in the ranges of 150-250, 250-355 and 355-500 μm. The pore walls of the PLGA sponges were connected with each other as an integral and continuous structure. Removal of the integral and continuous templating PLGA left negative replica spaces (highlighted red in the images

of Figure 2.1c) in the collagen scaffolds, which formed interconnecting channels in the scaffolds. The interconnecting channels were linked with the pores of collagen microsponges, making all the pores well interconnected. The interconnecting channels in the collagen scaffolds were large when the PLGA sponges prepared with 10 wt.% PLGA and large salt particulates were used as templates, and the well-interconnected pore structures may facilitate homogenous cell distribution throughout the scaffolds.

2.6 Conclusions

Collagen scaffolds with high interconnectivity were prepared using sacrificial PLGA sponge templates. The pore structure of the collagen scaffolds was controlled by the porosity and pore size of the sacrificial PLGA sponges. These collagen scaffolds, in particular the Col-10-355 scaffold, had high interconnectivity with large interconnecting channels throughout the scaffolds.

2.7 References

[1] R. Wu, Y. Li, M. Shen, X. Yang, L. Zhang, X. Ke, G. Yang, C. Gao, Z. Gou, S. Xu, Bone tissue regeneration: the role of finely tuned pore architecture of bioactive scaffolds before clinical translation, Bioactive materials 6(5) (2021) 1242-1254.
[2] W. Li, Y. Bai, J. Cao, S. Gao, P. Xu, G. Feng, L. Wang, H. Wang, D. Kong, M. Fan, Highly interconnected inverse opal extracellular matrix scaffolds enhance stem cell therapy in limb ischemia, Acta Biomaterialia 128 (2021) 209-221.
[3] A. Wubneh, E.K. Tsekoura, C. Ayranci, H. Uludağ, Current state of fabrication technologies and materials for bone tissue engineering, Acta Biomaterialia 80 (2018) 1-30.
[4] Y. Chen, K. Lee, N. Kawazoe, Y. Yang, G. Chen, PLGA–collagen–ECM hybrid scaffolds functionalized with biomimetic extracellular matrices secreted by mesenchymal stem cells during stepwise osteogenesis-co-adipogenesis, Journal of Materials Chemistry B 7(45) (2019) 7195-7206.
[5] K. Lee, Y. Chen, X. Li, Y. Wang, N. Kawazoe, Y. Yang, G. Chen, Solution viscosity regulates chondrocyte proliferation and phenotype during 3D culture, J Mater Chem B 7(48) (2019) 7713-7722.
[6] P. Bajaj, R.M. Schweller, A. Khademhosseini, J.L. West, R. Bashir, 3D biofabrication strategies for tissue engineering and regenerative medicine, Annual review of biomedical engineering 16 (2014) 247-276.
[7] S. Reed, G. Lau, B. Delattre, D.D. Lopez, A.P. Tomsia, B.M. Wu, Macro-and micro-designed chitosan-alginate scaffold architecture by three-dimensional printing and directional freezing, Biofabrication 8(1) (2016) 015003.
[8] M. Simonet, N. Stingelin, J.G. Wismans, C.W. Oomens, A. Driessen-Mol, F.P. Baaijens, Tailoring the void space and mechanical properties in electrospun scaffolds towards physiological ranges, Journal of Materials Chemistry B 2(3) (2014) 305-313.
[9] T.G. Kim, H.J. Chung, T.G. Park, Macroporous and nanofibrous hyaluronic acid/collagen hybrid scaffold fabricated by concurrent electrospinning and deposition/leaching of salt particles, Acta Biomaterialia 4(6) (2008) 1611-9.
[10] L. Sutrisno, H. Chen, Y. Chen, T. Yoshitomi, N. Kawazoe, Y. Yang, G. Chen, Composite scaffolds of black phosphorus nanosheets and gelatin with controlled pore structures for photothermal cancer therapy and adipose tissue engineering, Biomaterials (2021) 120923.
[11] Q. Zhang, H. Lu, N. Kawazoe, G. Chen, Pore size effect of collagen scaffolds on cartilage regeneration, Acta Biomaterialia 10(5) (2014) 2005-13.
[12] H. Zhang, I. Hussain, M. Brust, M.F. Butler, S.P. Rannard, A.I. Cooper, Aligned two-and three-dimensional structures by directional freezing of polymers and nanoparticles, Nature Materials 4(10) (2005) 787-793.
[13] K. Qin, C. Parisi, F.M. Fernandes, Recent advances in ice templating: from biomimetic composites to cell culture scaffolds and tissue engineering, Journal of Materials Chemistry B 9(4) (2021) 889-907.
[14] Y.S. Zhang, C. Zhu, Y. Xia, Inverse opal scaffolds and their biomedical applications, Advanced Materials 29(33) (2017) 1701115.
[15] D. Huang, T. Liu, J. Liao, S. Maharjan, X. Xie, M. Pérez, I. Anaya, S. Wang, A.T. Mayer, Z. Kang, Reversed-engineered human alveolar lung-on-a-chip model, Proceedings of the National Academy of Sciences 118(19) (2021).
[16] K.-y. Chung, N.C. Mishra, C.-c. Wang, F.-h. Lin, K.-h. Lin, Fabricating scaffolds by microfluidics, Biomicrofluidics 3(2) (2009) 022403.
[17] C.-C. Wang, K.-C. Yang, K.-H. Lin, H.-C. Liu, F.-H. Lin, A highly organized three-dimensional alginate scaffold for cartilage tissue engineering prepared by microfluidic technology, Biomaterials 32(29) (2011) 7118-7126.
[18] P. Zhao, J. Wang, Y. Li, X. Wang, C. Chen, G. Liu, Microfluidic Technology for the Production of Well-Ordered Porous Polymer Scaffolds, Polymers 12(9) (2020) 1863.
[19] H. Zreiqat, Y. Ramaswamy, C. Wu, A. Paschalidis, Z. Lu, B. James, O. Birke, M. McDonald, D. Little, C.R. Dunstan, The incorporation of strontium and zinc into a calcium–silicon ceramic for bone tissue engineering, Biomaterials 31(12) (2010) 3175-3184.
[20] R.T. Tran, E. Naseri, A. Kolasnikov, X. Bai, J. Yang, A new generation of sodium chloride porogen for tissue engineering, Biotechnology and Applied Biochemistry 58(5) (2011) 335-344.

Chapter 3

Three-dimensional culture of chondrocytes in the porous collagen scaffolds for cartilage tissue engineering

3.1 Abstract

Chondrocytes isolated from patient cartilage biopsy are expanded *in vitro* and used for cartilage tissue engineering. In this part, bovine articular chondrocytes were seeded in the collagen scaffolds with interconnected pore structures for cartilage tissue engineering. Chondrocytes maintained high viability in all the PLGA-templated collagen scaffolds and the control scaffold. Nuclear staining showed that cells were densely distributed on the scaffold surface of the control collagen scaffold and fewer cells were distributed in the central regions. After 6 weeks of *in vitro* culture, the cell/scaffold constructs formed in the PLGA-templated collagen scaffolds had significantly higher Young's moduli than that formed in the control collagen scaffold. PLGA-templated collagen scaffolds promoted chondrocytes proliferation and sGAG secretion comparing with control scaffold. Chondrocytes cultured in the PLGA-templated collagen scaffolds expressed significantly higher levels of collagen type II and aggrecan genes than the cells cultured in the control collagen scaffold.

3.2 Introduction

Articular cartilage is avascular, aneural and alymphatic tissue with limited spontaneous healing capability [1-3]. Damaged articular cartilage leads to joint pain, immobility and breakdown, which can impair patient quality of life [4-6]. Due to the problems of traditional treatments such as microfracture and mosaicplasty, cartilage tissue engineering has been developed as a promising strategy for cartilage regeneration and joint function restoration [1, 7]. Three-dimensional (3D) scaffolds play an important role in cartilage tissue engineering because they can provide essential support for cell adhesion, proliferation, the secretion of extracellular matrix and cartilage formation [8-12]. Cartilage tissue engineering requires homogeneous cell distribution throughout the scaffolds to guarantee the regeneration of functional cartilage tissue [13-15]. Nonhomogeneous cell distribution may result in defects in the engineered tissues where void spaces are formed in regions without cells [16].

Bovine articular chondrocytes were cultured in collagen scaffolds to investigate the influence of their pore structures on cell distribution, cell proliferation, matrix secretion and cartilage tissue regeneration.

3.3 Materials and methods

3.3.1 Culture of chondrocytes in collagen scaffolds

The collagen scaffolds were punched into discs with a diameter of 6 mm and a thickness of 3 mm for cell culture. The scaffold discs were sterilized with 70% ethanol for 30 minutes and washed with PBS 3 times and Dulbecco's modified Eagle's medium (DMEM, Sigma-Aldrich) once. Sterile silicone frames with holes 6 mm in diameter were used to constrain the cell suspension solution in the scaffold discs. The sterilized and medium-impregnated scaffold discs were put into the holes of silicone frames, and excess medium was removed, making the scaffold discs ready for cell seeding. Bovine articular chondrocytes were isolated from the articular cartilage of the knees of a 9-week-old female calf, which were purchased from a local slaughterhouse as previously reported [17]. The isolated chondrocytes were cultured in 175 cm^2 tissue culture flasks in DMEM supplemented with 10% fetal bovine serum, 4500 mg L^{-1} glucose, 100 U mL^{-1} penicillin, 4 mM glutamine, 1 mM sodium pyruvate, 0.4 mM proline, 100 mg mL^{-1} streptomycin, 0.1 mM nonessential amino acids and 50 mg mL^{-1} ascorbic acid at 37 °C in 5% CO_2. After three passages, chondrocytes were harvested and resuspended in culture medium at 1.5×10^7 cells mL^{-1} for cell seeding. Then, 100 µL of cell suspension was dropped on top of scaffold discs and cultured at 37 °C in 5% CO_2. After culturing for 6 hours, the scaffold discs were turned upside down, and another 100 µL of cell suspension was dropped on the other side of the scaffolds (200 µL cell suspension, 3×10^6 cell/scaffold). The cell/scaffold constructs in the silicone frames were cultured for another 6 hours and then moved into 75 cm^2 tissue culture flasks for continual culture under shaking at 60 rpm. The medium was changed every three days.

3.3.2 Nuclear staining of chondrocytes in collagen scaffolds

After culture for one day, the cell distribution in the scaffolds was examined by nuclear staining. After one day of culture, the cell/scaffold constructs were washed with PBS three times and fixed with 10% neutral buffered formalin (FUJIFILM Wako Pure Chemical) for 24 hours at room temperature. The fixed cell/scaffold constructs were dehydrated, embedded in paraffin and sliced to obtain vertical cross-sections at a thickness of 7 µm. The slices were incubated with 1 µg mL^{-1} 4',6-diamidino-2-phenylindole dihydrochloride (DAPI, Dojindo Laboratories, Kumamoto, Japan) for 10 minutes to stain the nuclei of the chondrocytes. The stained cross-sections were observed with a fluorescence microscope (Olympus, Tokyo, Japan).

3.3.3 Quantification of DNA and sulfated glycosaminoglycan (sGAG) and compression test

DNA and sGAG were quantified after culture for 1 day, 2 weeks, 4 weeks and 6 weeks. The cell/scaffold constructs were washed with PBS 3 times, freeze-dried and digested with papain solution for 6 hours at 60 °C under shaking. The papain solution was prepared by dissolving papain (Sigma-Aldrich, St Louis, Missouri, USA) at 400 µg/mL in sterile 0.1 M phosphate buffer with 5 mM L-cysteine hydrochloride monohydrate (Sigma-Aldrich) and 5 mM ethylenediaminetetraacetic acid disodium salt dihydrate (EDTA-2Na, Sigma-Aldrich) at a pH of 6. The papain-digested solution was used to measure the DNA amount with Hoechst 33258 (Sigma-Aldrich) using a spectrofluorometer

(FP8500, JASCO, Tokyo, Japan). sGAG was quantified by using a Blyscan™ Glycosaminoglycan Assay Kit (Biocolor, County Antrim, UK). Three samples of each group at each time point were used for the measurements. The cell/scaffold constructs after culture for 6 weeks were washed with PBS three times and used for the compression test, which was carried out as described above. Three samples of each group were measured.

3.3.4 Real-time PCR

After 6 weeks of culture, the cell/scaffold constructs were washed with PBS, frozen in liquid nitrogen and pulverized into powders using an electric crusher. The powders of each sample were digested with 1 mL of Sepasol-RNA I Super G solution (Nacalai Tesque, Kyoto, Japan) and total RNA was extracted as previously reported [18]. Reverse transcription from RNA to cDNA was performed using a high-capacity cDNA reverse transcription kit (Thermo Fisher Scientific). Real-time PCR was performed to amplify glyceraldehyde-3-phosphate dehydrogenase (GAPDH, a housekeeping gene), collagen type I (Col1a2), collagen type II (Col2a1) and aggrecan (Acan) using a QuantStudio® 3 Real-Time PCR System (Thermo Fisher Scientific) with previously reported primer and probe sequences [19]. Relative gene expression was calculated with the $2^{-\Delta\Delta Ct}$ method by using GAPDH as an endogenous control. Data were normalized to the expression of the respective genes of the cells cultured in the control collagen scaffold. Three samples of each group were used for the analysis (n = 3).

3.3.5 Histological and immunohistochemical staining

After 6 weeks of culture, the cell/scaffold constructs were washed with PBS 3 times and fixed with 10% neutral buffered formalin for 24 hours at room temperature. The fixed cell/scaffold constructs were dehydrated, embedded in paraffin and sliced by a microtome to obtain cross-sections at a thickness of 7 μm. The cross-sections were stained with safranin O/light green. In addition, immunohistochemistry was performed to visualize collagen type II, collagen type I and aggrecan. Epitopes in the cross-sections were retrieved by treatment with proteinase K for 10 minutes. The cross-sections were blocked with peroxidase blocking solution and 10% goat serum solution for 5 and 30 minutes, respectively. Then, they were incubated with primary antibody (rabbit polyclonal anti-collagen type II (AB746; Merck Millipore, Burlington, MA, USA), rabbit polyclonal anti-aggrecan (PA1-1746; Thermo Scientific) and rabbit monoclonal anti-collagen type I (PA1-26204; Thermo Scientific, Rockford, IL, USA)) at a 1:100 working dilution overnight at 4 °C. Next, the cross-sections were incubated with secondary antibody (peroxidase-labeled polymer-conjugated secondary antibody (DakoCytomation Envision+; Agilent, Santa Clara, CA, USA)) for 30 minutes at room temperature. Finally, the color was developed by using 3,3'-diaminobenzidine (DAB; Liquid DAB+ Substrate Chromogen System, Agilent) for 10 minutes and observed under an optical microscope (Olympus).

3.3.6 Statistical analysis

All quantitative analysis experiments were performed in triplicate. One-way analysis of variance (ANOVA) was used to calculate the significance of all the data using KyPlot 5.0 (KyensLab Inc., Tokyo, Japan). The results are reported as the mean ± standard deviation (SD). Significant differences

are shown as * ($p < 0.05$), ** ($p < 0.01$) and *** ($p < 0.001$).

3.4 Results

3.4.1 Cell viability, distribution and adhesion in the collagen scaffolds

Bovine articular chondrocytes were seeded in the PLGA-templated collagen scaffolds and control scaffold. The cell seeding efficiency of all the scaffolds was higher than 95% (Table 1), which indicated that most of the cells were successfully seeded into the scaffolds. The cell seeding efficiency was not significantly different between the PLGA-templated collagen scaffolds and the control collagen scaffold. The cell seeding method using silicone frames could protect against cell leakage during cell seeding and allowed most of the cells to adhere on or in the scaffolds.

Cell viability, distribution and adhesion were evaluated after one day of culture. Live/dead staining showed that almost all the chondrocytes were alive and very few were dead, which indicated that chondrocytes maintained high viability in all the PLGA-templated collagen scaffolds and the control scaffold (Figure 3.1a). Cell distribution in the scaffolds was visualized by staining cell nuclei in the sections of cell/scaffold constructs with DAPI (Figure 3.1b). Nuclear staining showed that cells were densely distributed on the scaffold surface of the control collagen scaffold and fewer cells were distributed in the central regions. On the other hand, cells were more homogeneously distributed in the PLGA-templated collagen scaffolds. From the top surface to the central region and bottom region, cells were detected at almost the same frequency. The dark holes in the central regions indicated the pores of the scaffolds and the cells were distributed on the pore walls. The good interconnectivity of the PLGA-templated collagen scaffolds facilitated cell penetration and resulted in homogenous cell distribution throughout the scaffolds. Among all the collagen scaffolds, the cell distribution was most homogeneous in the collagen scaffolds templated by the PLGA sponge templates formed with 10 wt.% PLGA and large salt particulates. This should be due to the large interconnecting channels in these collagen scaffolds, as shown in Fig. 1b. SEM observation indicated that the cells adhered to all the scaffolds (Figure 3.1c). The pore structures of the scaffolds remained unchanged after one day of cell culture.

3.4.2 Gross appearance and mechanical property of engineered cartilage tissue

Bovine articular chondrocytes were cultured *in vitro* in collagen scaffolds for 6 weeks. The engineered cartilage tissue after 6 weeks culture showed white glossing appearance (Fig. 4a). They showed the same round disc structure as those of the collagen scaffold discs except the control. The shape of the control scaffold changed. The size of engineered cartilage tissue using all the PLGA-templated collagen scaffolds was almost the same as that of the scaffolds.

The Young's moduli of the engineered cartilage tissue were measured by a compressive test (Fig. 4b). The cell/scaffold constructs formed in the PLGA-templated collagen scaffolds had significantly higher Young's moduli than that formed in the control collagen scaffold. The cell/scaffold constructs formed in Col-10-250 and Col-10-355 had significantly higher Young's moduli than that formed in Col-5-150. The Young's moduli of cell/scaffold constructs increased in the collagen scaffolds templated by the PLGA sponges prepared with 10 wt.% PLGA and large salt particulates. By simple subtraction of the compression modulus of the respective hydrated scaffolds, the tissues formed in the

Col-10-150, Col-10-250 and Col-10-355 scaffolds had a higher compression modulus than those formed in the other scaffolds, particularly the control collagen scaffold.

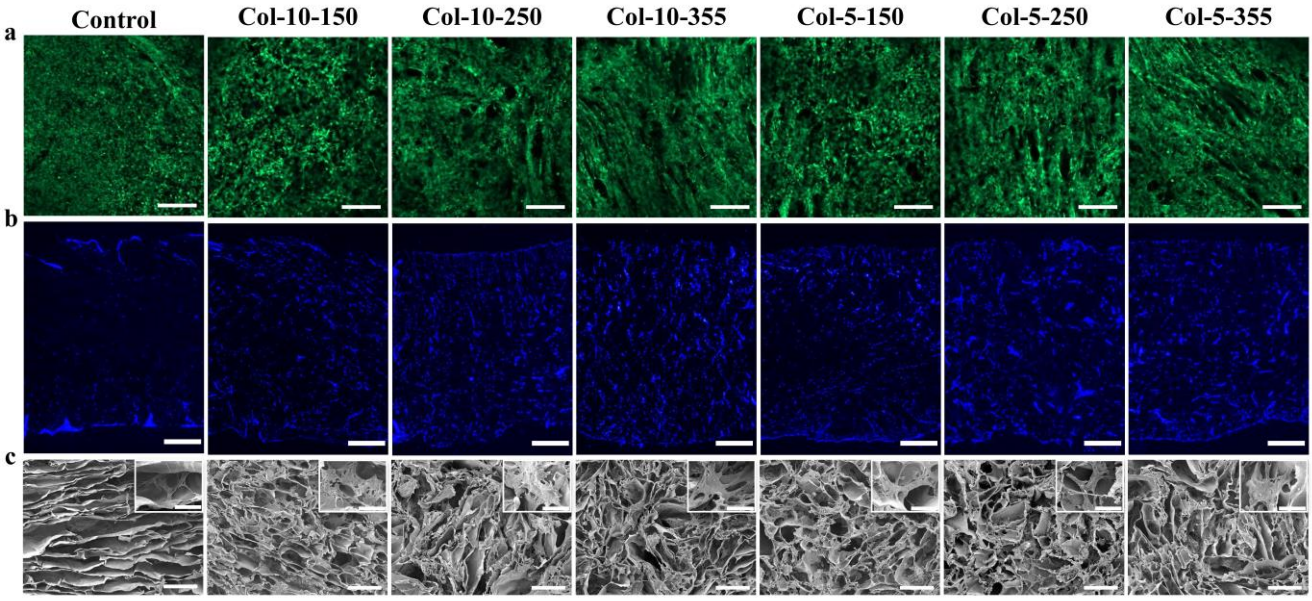

Figure 3.1 (a) Staining of live and dead chondrocytes cultured in PLGA-templated collagen scaffolds and control scaffold for 1 day. Live cells were stained green and dead cells were stained red. Scale bar: 200 μm. (b) Nuclear staining of chondrocytes cultured in the scaffolds for 1 day. Cell nuclei were stained blue. Scale bar: 500 μm. (c) SEM images of the cross-sections of the cell/scaffold constructs after 1 day of culture. Scale bar: 200 μm. The inserts show the magnified SEM images. Scale bar: 50 μm.

3.4.3 Quantification of DNA and sGAG in the cell/scaffold constructs

The DNA amount in the cell/scaffold constructs was measured to evaluate cell proliferation after culture for 1 day, 2 weeks, 4 weeks and 6 weeks (Figure 3.3a). Chondrocytes proliferated in all the scaffolds during 6 weeks of culture. The DNA amounts in the PLGA-templated collagen scaffolds were significantly higher than that in the control collagen scaffold after 2, 4 and 6 weeks of culture. Furthermore, the DNA amount increased when the cells were cultured in the collagen scaffolds templated by PLGA sponges prepared with 10 wt.% PLGA and large salt particulates. The results indicated that the collagen scaffolds templated by the PLGA sponges prepared with 10 wt.% PLGA and large salt particulates were more beneficial for cell proliferation than the other scaffolds.

Quantification of sGAG showed that the sGAG amount increased during cell culture for all the scaffolds (Figure 3.3b). Chondrocytes secreted significantly more sGAG in the Col-10-150, Col-10-250 and Col-10-355 scaffolds than in the respective Col-5-150, Col-5-250 and Col-5-355 scaffolds. The collagen scaffolds templated by the PLGA sponges prepared with large salt particulates promoted sGAG secretion more strongly than those prepared from small salt particulates.

The amount of sGAG was normalized to the DNA amount (Figure 3.3c). The sGAG/DNA ratio was not significantly different among all the scaffolds after culture for 1 day and 2 weeks. However, after culture for 4 and 6 weeks, the sGAG/DNA ratio in the PLGA-templated collagen scaffolds was significantly higher than that in the control collagen scaffold. The sGAG/DNA ratio increased when chondrocytes were cultured in collagen scaffolds templated by PLGA sponges prepared with 10 wt.%

PLGA and large salt particulates.

These results suggested that the collagen scaffolds supported chondrocyte proliferation and promoted ECM production. The collagen scaffolds templated by the PLGA sponges prepared with 10 wt.% PLGA and large salt particulates were favorable for cell proliferation and the production of cartilaginous ECM.

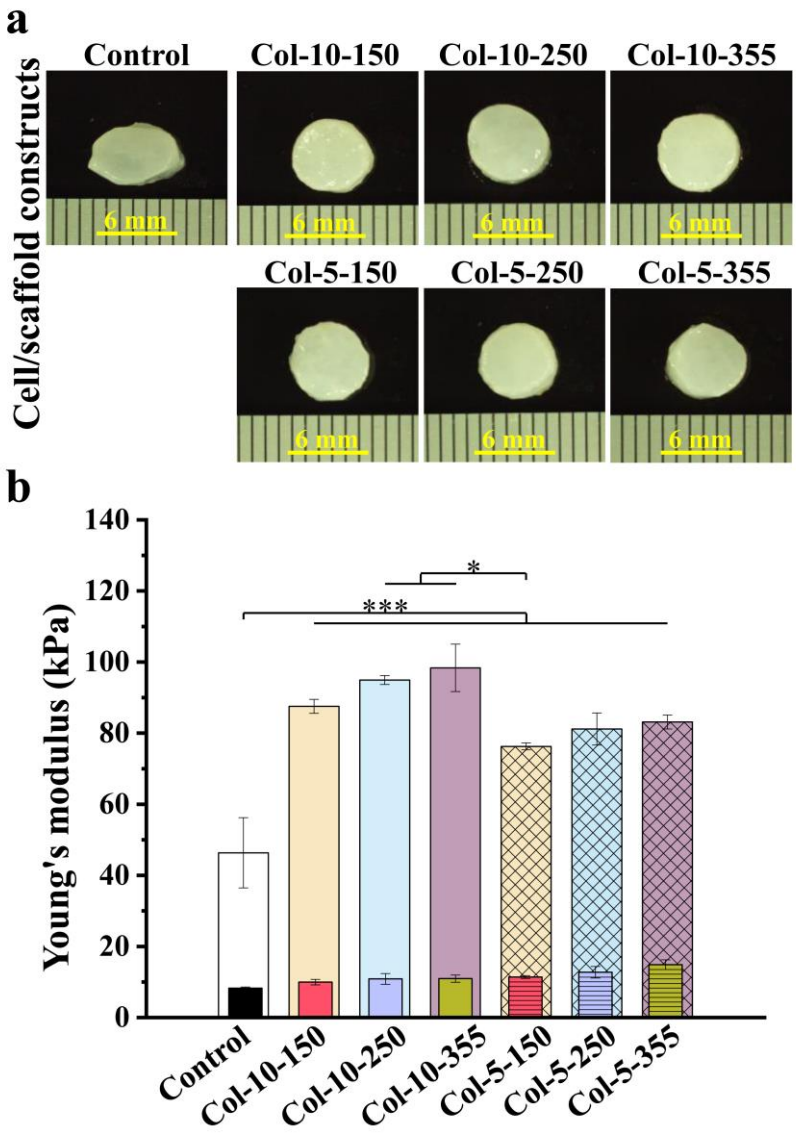

Figure 3.2 (a) Photomicrographs and (b) compression moduli of the cell/scaffold constructs after in vitro culture for 6 weeks. The Young's moduli of the respective hydrated collagen scaffolds before cell culture are shown with the inserted narrow columns. Data represent mean ± SD, n = 3. Significant difference: *, $p < 0.05$; ***, $p < 0.001$.

3.4.4 Expression of cartilaginous genes

Collagen type II and aggrecan are two specific markers of articular chondrocytes, while collagen type I is a marker of dedifferentiation articular chondrocytes. The gene expression level of these three genes was analyzed by real-time RT-PCR after chondrocytes were cultured in the scaffolds for 6 weeks (Figure 3.4). The expression level of collagen type I was not significantly different among the PLGA-

templated collagen scaffolds and the control collagen scaffold. However, chondrocytes cultured in the PLGA-templated collagen scaffolds expressed significantly higher levels of collagen type II and aggrecan genes than chondrocytes cultured in the control collagen scaffold. Chondrocytes expressed higher levels of collagen type II and aggrecan genes in the Col-10-150, Col-10-250 and Col-10-355 scaffolds than in the Col-5-150, Col-5-250 and Col-5-355 scaffolds. The expression levels of these two genes increased when chondrocytes were cultured in the collagen scaffolds templated by PLGA sponges prepared with large salt particulates.

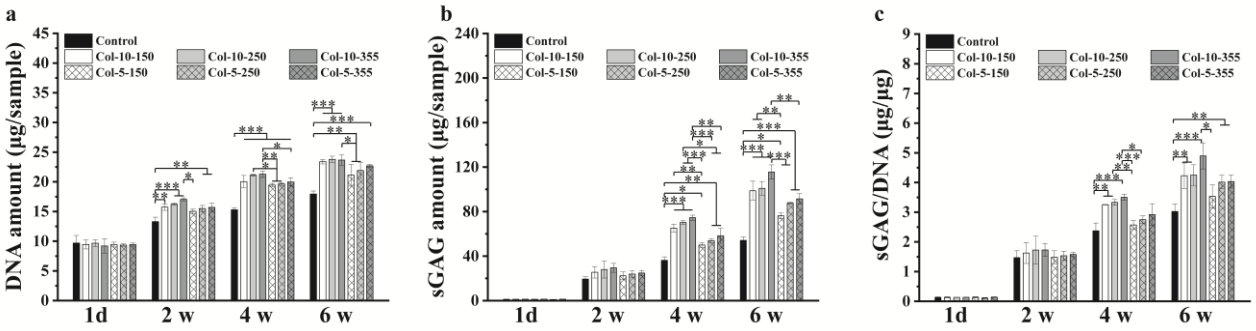

Figure 3.3 (a) DNA amount, (b) sGAG amount and (c) sGAG/DNA ratio in the cell/scaffold constructs after in vitro culture for 6 weeks. Data represent mean ± SD, n = 3. Significant difference: *, $p < 0.05$; **, $p < 0.01$; ***, $p < 0.001$.

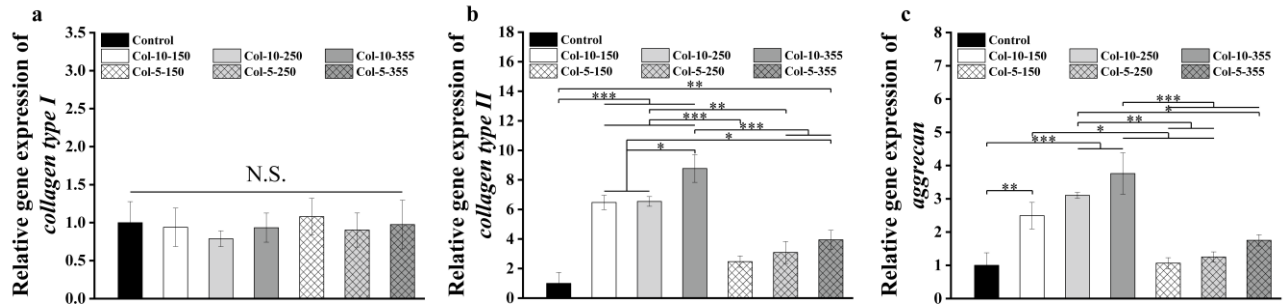

Figure 3.4 Gene expression profiles of (a) collagen type I, (b) collagen type II and (c) aggrecan of chondrocytes cultured in the PLGA-templated collagen scaffolds and control collagen scaffolds for 6 weeks. Data were normalized to the expression of the respective genes of the chondrocytes cultured in the control collagen scaffold. Data represent mean ± SD, n = 3. Significant difference: *, $p < 0.05$; **, $p < 0.01$; ***, $p < 0.001$.

3.4.5 Histological and immunohistochemical staining

Histological and immunohistochemical staining were carried out to investigate the secretion and distribution of cartilaginous extracellular matrix after *in vitro* culture for 6 weeks. Safranin O staining showed abundant cartilaginous extracellular matrix throughout the PLGA-templated collagen scaffolds and sparse cartilaginous extracellular matrix in the control collagen scaffold. Immunohistochemical staining showed that collagen type II and aggrecan were more strongly stained and more homogeneously distributed in the PLGA-templated collagen scaffolds than in the control

collagen scaffold. Their staining intensity was highest in the collagen scaffolds templated by the PLGA sponges prepared with 10 wt.% PLGA and large salt particulates. However, the immunohistochemical staining intensity of collagen type I was very weak for all the scaffolds. The results indicated that the PLGA-templated collagen scaffolds, in particular the collagen scaffolds templated by the PLGA sponges prepared with 10 wt.% PLGA and large salt particulates, facilitated the secretion of cartilaginous extracellular matrix and its homogenous distribution throughout the scaffolds.

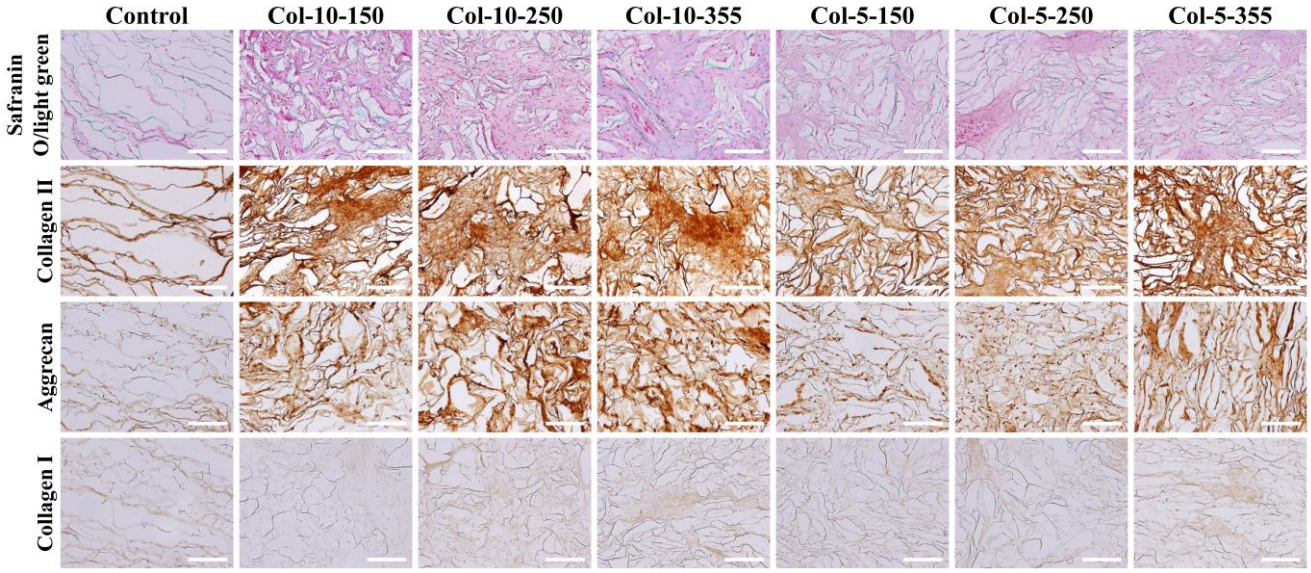

Figure 3.5 Safranin O staining and immunohistochemical staining of collagen type II, aggrecan and collagen type I in the cell/scaffold constructs after in vitro culture for 6 weeks. Scale bar: 200 μm.

3.5 Discussion

The seeded chondrocytes could penetrate from the scaffold surface to the inner pores through the interconnecting channels. The cell distribution was more homogenous in the collagen scaffolds templated by the PLGA sponges prepared with a high PLGA/NaCl ratio and large salt particulates. Of all the scaffolds, the cell distribution was most homogenous in the Col-10-355 scaffold because the interconnecting channels in the scaffold were the largest.

The proliferation, sGAG quantification, gene expression, histological staining and immunohistochemical staining results indicated that chondrocytes in the PLGA-templated collagen scaffolds, particularly Col-10-355, proliferated fast, expressed higher levels of cartilaginous genes and secreted more cartilaginous extracellular matrices. These results could be explained by the more homogenous cell distribution in these scaffolds. The homogeneous cell distribution allowed the cells to adhere to the pore walls and proliferate quickly to occupy the spaces of all the pores. The rapidly proliferating chondrocytes could form aggregates in the pores of collagen scaffolds, thereby promoting the expression of collagen type II and aggrecan and the secretion of cartilaginous extracellular matrix. However, the chondrocytes seeded in the control collagen scaffold accumulated mainly on the surface of the scaffold, which resulted in the formation of dense tissue on the scaffold surface and many void spaces inside the control collagen scaffold. Therefore, the control collagen scaffold showed inhomogeneous formation of the cell/scaffold construct after 6 weeks of culture, low expression of collagen type II and aggrecan and low secretion of cartilaginous extracellular matrix. It has been reported that the aggregates or spheroids of chondrocytes promote the expression of cartilaginous

genes and the secretion of cartilaginous extracellular matrix [20-22]. In addition, good pore interconnectivity can facilitate nutrient transport and waste removal to supply sufficient nutrients inside the scaffolds [23-25]. However, the dominant cell distribution on the surface of the control collagen scaffold caused overpopulation on the scaffold surface, which might result in fewer cell-cell interactions and limit nutrient supply in the inner regions of the control collagen scaffold [23]. The homogenous tissue formation in the PLGA-templated collagen scaffolds, in particular Col-10-355, resulted in higher compression strength of the regenerated tissues in these scaffolds (Fig. 4b).

Pore structures have different influences on cell functions through direct or indirect interactions with cells. Pore structures have been reported to directly affect cell adhesion, distribution, proliferation and differentiation and matrix secretion and distribution [24]. They have also been reported to affect mechanical properties and release of bioactive molecules, which in turn affect cell functions and tissue regeneration [16, 25]. Pore interconnectivity can affect not only cell distribution but also tissue infiltration, bone tissue regeneration and angiogenesis [26-28]. Porogens with defined shapes and sizes have been used as sacrificial templates to control pore size and interconnectivity [12, 29-32]. Methods using microsphere templates, air bubbles or liquid droplets have been used to precisely control the pore structures of porous scaffolds [33-36]. However, the microspheres, air bubbles or liquid droplets must be bound and connected before creating pore structures. When *ccp* lattices of monodispersed microspheres are used as sacrificial templates to prepare inverse opal scaffolds, the microspheres need to be pretreated with heat or other binding methods to allow the contact points of the microbeads to be bound and the structure is essential to create interconnectivity in the template-derived pore structures [29, 30]. However, the PLGA sponge templates in this study had an integral and continuous templating structure and did not need any other pretreatments. The integral structures of the PLGA templates could introduce a completely interconnected pore structure throughout the collagen scaffolds without any defects. The PLGA-templated collagen scaffolds promoted cell proliferation, secretion of cartilaginous matrices and regeneration of cartilage tissue. They should be useful for cartilage tissue engineering.

3.6 Conclusions

Chondrocytes adhered and distributed homogeneously in the collagen scaffolds and showed a high proliferation rate, high expression of cartilaginous genes and secretion of cartilaginous extracellular matrix. The collagen scaffolds, in particular, Col-10-355, facilitated the formation of homogenous tissue with high compression strength. The method using PLGA sponges as sacrificial templates should open a new avenue for the preparation of well-interconnected pore scaffolds for cartilage tissue engineering.

3.7 References

[1] H. Kwon, W.E. Brown, C.A. Lee, D. Wang, N. Paschos, J.C. Hu, K.A. Athanasiou, Surgical and tissue engineering strategies for articular cartilage and meniscus repair, Nat Rev Rheumatol 15(9) (2019) 550-570.
[2] M.P. Murphy, L.S. Koepke, M.T. Lopez, X. Tong, T.H. Ambrosi, G.S. Gulati, O. Marecic, Y. Wang, R.C. Ransom, M.Y. Hoover, H. Steininger, L. Zhao, M.P. Walkiewicz, N. Quarto, B. Levi, D.C. Wan, I.L. Weissman, S.B. Goodman, F. Yang, M.T. Longaker, C.K.F. Chan, Articular cartilage regeneration by activated skeletal stem cells, Nat Med 26(10) (2020) 1583-1592.
[3] A.R. Armiento, M. Alini, M.J. Stoddart, Articular fibrocartilage - Why does hyaline cartilage fail to repair?, Adv Drug Deliv Rev 146 (2019) 289-305.
[4] R.N. Shah, N.A. Shah, M.M. Del Rosario Lim, C. Hsieh, G. Nuber, S.I. Stupp, Supramolecular design of self-assembling nanofibers for cartilage regeneration, Proc Natl Acad Sci U S A 107(8) (2010) 3293-8.
[5] M. Farokhi, F. Jonidi Shariatzadeh, A. Solouk, H. Mirzadeh, Alginate Based Scaffolds for Cartilage Tissue Engineering: A Review, International Journal of Polymeric Materials and Polymeric Biomaterials 69(4) (2019) 230-247.
[6] Z. Zhao, C. Fan, F. Chen, Y. Sun, Y. Xia, A. Ji, D.A. Wang, Progress in Articular Cartilage Tissue Engineering: A Review on Therapeutic Cells and Macromolecular Scaffolds, Macromolecular Bioscience 20(2) (2020) e1900278.
[7] B.A.G. Melo, Y.A. Jodat, S. Mehrotra, M.A. Calabrese, T. Kamperman, B.B. Mandal, M.H.A. Santana, E. Alsberg, J. Leijten, S.R. Shin, 3D Printed Cartilage‐Like Tissue Constructs with Spatially Controlled Mechanical Properties, Advanced Functional Materials 29(51) (2019).
[8] C.a. Chen, K. Huang, J. Zhu, Y. Bi, L. Wang, J. Jiang, T. Zhu, X. Yan, J. Zhao, A novel elastic and controlled-release poly (ether-ester-urethane) urea scaffold for cartilage regeneration, Journal of Materials Chemistry B 8(18) (2020) 4106-4121.
[9] S. Chen, J.V. John, A. McCarthy, J. Xie, New forms of electrospun nanofiber materials for biomedical applications, Journal of Materials Chemistry B 8(17) (2020) 3733-3746.
[10] B. Zhang, J. Huang, R.J. Narayan, Gradient scaffolds for osteochondral tissue engineering and regeneration, Journal of Materials Chemistry B 8(36) (2020) 8149-8170.
[11] G. Chen, T. Sato, T. Ushida, N. Ochiai, T. Tateishi, Tissue engineering of cartilage using a hybrid scaffold of synthetic polymer and collagen, Tissue engineering 10(3-4) (2004) 323-330.
[12] H. Lu, Y.G. Ko, N. Kawazoe, G. Chen, Cartilage tissue engineering using funnel-like collagen sponges prepared with embossing ice particulate templates, Biomaterials 31(22) (2010) 5825-35.
[13] S. Miot, T. Woodfield, A.U. Daniels, R. Suetterlin, I. Peterschmitt, M. Heberer, C.A. Van Blitterswijk, J. Riesle, I. Martin, Effects of scaffold composition and architecture on human nasal chondrocyte redifferentiation and cartilaginous matrix deposition, Biomaterials 26(15) (2005) 2479-2489.
[14] T. Lam, T. Dehne, J.P. Krüger, S. Hondke, M. Endres, A. Thomas, R. Lauster, M. Sittinger, L. Kloke, Photopolymerizable gelatin and hyaluronic acid for stereolithographic 3D bioprinting of tissue‐engineered cartilage, Journal of Biomedical Materials Research Part B: Applied Biomaterials 107(8) (2019) 2649-2657.
[15] X. Feng, P. Xu, T. Shen, Y. Zhang, J. Ye, C. Gao, Influence of pore architectures of silk fibroin/collagen composite scaffolds on the regeneration of osteochondral defects in vivo, Journal of Materials Chemistry B 8(3) (2020) 391-405.
[16] S. Chen, Q. Zhang, T. Nakamoto, N. Kawazoe, G. Chen, Gelatin Scaffolds with Controlled Pore Structure and Mechanical Property for Cartilage Tissue Engineering, Tissue Eng Part C Methods 22(3) (2016) 189-98.
[17] Q. Zhang, H. Lu, N. Kawazoe, G. Chen, Pore size effect of collagen scaffolds on cartilage regeneration, Acta Biomaterialia 10(5) (2014) 2005-13.
[18] Y. Chen, K. Lee, Y. Yang, N. Kawazoe, G. Chen, PLGA-collagen-ECM hybrid meshes mimicking stepwise osteogenesis and their influence on the osteogenic differentiation of hMSCs, Biofabrication 12(2) (2020) 025027.
[19] K. Lee, Y. Chen, X. Li, Y. Wang, N. Kawazoe, Y. Yang, G. Chen, Solution viscosity regulates chondrocyte proliferation and phenotype during 3D culture, J Mater Chem B 7(48) (2019) 7713-7722.
[20] M.M. Nava, L. Draghi, C. Giordano, R. Pietrabissa, The effect of scaffold pore size in cartilage tissue engineering, Journal of applied biomaterials & functional materials 14(3) (2016) e223-e229.
[21] N.P. Grigull, J.I. Redeker, B. Schmitt, M.M. Saller, V. Schönitzer, S. Mayer-Wagner, Chondrogenic potential of pellet culture compared to high-density culture on a bacterial cellulose hydrogel, International journal of molecular sciences 21(8) (2020) 2785.
[22] X. Yu, Y. Hu, L. Zou, S. Yan, H. Zhu, K. Zhang, W. Liu, D. He, J. Yin, A bilayered scaffold with

segregated hydrophilicity-hydrophobicity enables reconstruction of goat hierarchical temporomandibular joint condyle cartilage, Acta Biomaterialia 121 (2021) 288-302.
[23] J.W. Lee, G. Ahn, J.Y. Kim, D.W. Cho, Evaluating cell proliferation based on internal pore size and 3D scaffold architecture fabricated using solid freeform fabrication technology, J Mater Sci Mater Med 21(12) (2010) 3195-205.
[24] S.-M. Lien, L.-Y. Ko, T.-J. Huang, Effect of pore size on ECM secretion and cell growth in gelatin scaffold for articular cartilage tissue engineering, Acta Biomaterialia 5(2) (2009) 670-679.
[25] A. Szentivanyi, T. Chakradeo, H. Zernetsch, B. Glasmacher, Electrospun cellular microenvironments: Understanding controlled release and scaffold structure, Advanced Drug Delivery Reviews 63(4-5) (2011) 209-220.
[26] R. Dhandapani, P.D. Krishnan, A. Zennifer, V. Kannan, A. Manigandan, M.R. Arul, D. Jaiswal, A. Subramanian, S.G. Kumbar, S. Sethuraman, Additive manufacturing of biodegradable porous orthopaedic screw, Bioactive materials 5(3) (2020) 458-467.
[27] A.C. Jones, C.H. Arns, D.W. Hutmacher, B.K. Milthorpe, A.P. Sheppard, M.A. Knackstedt, The correlation of pore morphology, interconnectivity and physical properties of 3D ceramic scaffolds with bone ingrowth, Biomaterials 30(7) (2009) 1440-1451.
[28] S.W. Choi, Y. Zhang, M.R. MacEwan, Y. Xia, Neovascularization in biodegradable inverse opal scaffolds with uniform and precisely controlled pore sizes, Advanced healthcare materials 2(1) (2013) 145-154.
[29] Y.S. Zhang, C. Zhu, Y. Xia, Inverse opal scaffolds and their biomedical applications, Advanced Materials 29(33) (2017) 1701115.
[30] D. Huang, T. Liu, J. Liao, S. Maharjan, X. Xie, M. Pérez, I. Anaya, S. Wang, A.T. Mayer, Z. Kang, Reversed-engineered human alveolar lung-on-a-chip model, Proceedings of the National Academy of Sciences 118(19) (2021).
[31] N.C. Negrini, M. Bonnetier, G. Giatsidis, D.P. Orgill, S. Farè, B. Marelli, Tissue-mimicking gelatin scaffolds by alginate sacrificial templates for adipose tissue engineering, Acta Biomaterialia 87 (2019) 61-75.
[32] B.G. Ashinsky, S.E. Gullbrand, E.D. Bonnevie, C. Wang, D.H. Kim, L. Han, R.L. Mauck, H.E. Smith, Sacrificial fibers improve matrix distribution and micromechanical properties in a tissue-engineered intervertebral disc, Acta Biomaterialia 111 (2020) 232-241.
[33] P. Bajaj, R.M. Schweller, A. Khademhosseini, J.L. West, R. Bashir, 3D biofabrication strategies for tissue engineering and regenerative medicine, Annual review of biomedical engineering 16 (2014) 247-276.
[34] K.-y. Chung, N.C. Mishra, C.-c. Wang, F.-h. Lin, K.-h. Lin, Fabricating scaffolds by microfluidics, Biomicrofluidics 3(2) (2009) 022403.
[35] C.-C. Wang, K.-C. Yang, K.-H. Lin, H.-C. Liu, F.-H. Lin, A highly organized three-dimensional alginate scaffold for cartilage tissue engineering prepared by microfluidic technology, Biomaterials 32(29) (2011) 7118-7126.
[36] P. Zhao, J. Wang, Y. Li, X. Wang, C. Chen, G. Liu, Microfluidic Technology for the Production of Well-Ordered Porous Polymer Scaffolds, Polymers 12(9) (2020) 1863.

Chapter 4

Chondrogenic differentiation of mesenchymal stem cells in the porous collagen scaffolds

4.1 Abstract

Interconnected scaffolds are useful for promoting the chondrogenic differentiation of stem cells. The PLGA-templated collagen scaffolds were used to culture human bone marrow-derived mesenchymal stem cells (hMSCs) to investigate their promotive effect on the chondrogenic differentiation of hMSCs. The cells adhered to the scaffolds with a homogeneous distribution and proliferated with culture time. The expression of chondrogenesis-related genes was upregulated, and abundant cartilaginous matrices were detected. After subcutaneous implantation, the PLGA-templated collagen scaffolds further enhanced the production of cartilaginous matrices and the mechanical properties of the implants. The good interconnectivity of the PLGA-templated collagen scaffolds promoted chondrogenic differentiation. In particular, the collagen scaffolds prepared with large pore-bearing PLGA sponge templates showed the highest promotive effect.

4.2 Introduction

Cartilage tissue engineering has been developed as an attractive technique to heal cartilage defects [1, 2]. It has been broadly used for the regeneration of cartilage tissues to treat defects such as articular joint cartilage, nasal cartilage, auricular cartilage, tracheal cartilage, meniscus and intervertebral disc defects [3-6]. Different cell sources, such as chondrocytes and stem cells, are frequently used [7-9]. Chondrocytes isolated from patient cartilage biopsy are expanded *in vitro* and used for transplantation. The isolated chondrocytes have the advantages of a high level of matrix secretion and lack of hypertrophy. Autologous chondrocyte implantation has been clinically tried with good outcomes [10]. However, the use of chondrocytes relies on the availability of cartilage biopsy for chondrocyte isolation and involves chondrocyte dedifferentiation problems during *in vitro* expansion cultivation [11]. In addition to chondrocytes, stem cells, including bone marrow-derived mesenchymal stem cells (MSCs) and adipose-derived MSCs, are useful cell sources for the regeneration of cartilage tissues. [12]. Stem cells can be easily isolated and have high proliferation capacity and pluripotency [13-15]. When stem cells are used, chondrogenic differentiation to induce the stem cells to generate functional cartilage tissues is important [16].

Controlling cell functions such as the redifferentiation of dedifferentiated chondrocytes and chondrogenic differentiation of stem cells is pivotal for the regeneration of functional cartilage. A variety of factors and biomaterials have been investigated to control cell functions [17, 18]. As cell-supporting templates, scaffolds are critical for cartilage regeneration because they regulate cell adhesion, proliferation, matrix production and organization into functional tissues [19]. Scaffolds can provide a biomimetic microenvironment for three-dimensional (3D) cell culture and easy surgical handling [20]. Although pellet culture and hydrogel culture are attractive methods to induce chondrogenic differentiation and the redifferentiation of dedifferentiated

chondrocytes, 3D culture in porous scaffolds is a useful and important strategy for cartilage tissue engineering [2, 21]. In particular, porous scaffolds are useful for the regeneration of large and shaped cartilage tissues [22].

Scaffolds prepared from biodegradable polymers, including collagen, gelatin and hyaluronic acid, and their composites have been frequently applied for cartilage tissue engineering [23-25]. Collagen is a structural component of the cellular microenvironment and has specific cell adhesion ligands, such as RGD triple peptides [26]. It has been widely used for the preparation of many scaffolds for cartilage regeneration [27-29]. Porcine collagen I and collagen III collagen membranes and hyaluronic acid derivative polymer scaffolds have been used for scaffold-induced autologous chondrocyte implantation [30-32].

Porous scaffolds need to have well-interconnected pore structures for smooth cell seeding, homogeneous cell distribution and good cell–cell interactions. Many techniques have been established to prepare porous scaffolds with good interconnectivity [33, 34]. 3D printing, unidirectional freeze-drying, cubic close-packed lattices of microbeads and microfluidics are useful techniques for the fabrication of highly interconnected porous scaffolds [35, 36]. Except for pore interconnectivity, scaffolds should have high porosity to provide more space for accommodating large numbers of cells and facilitating cell–cell interactions [37, 38]. In our previous study, we prepared well-interconnected collagen porous scaffolds with high porosity using integral PLGA sponges as sacrificial templates [39]. The collagen scaffolds were highly interconnected and had high porosity. They facilitated cell seeding, adhesion, proliferation and cell–cell interactions. In this study, porous collagen scaffolds were applied for the 3D culture of human bone marrow-derived MSCs (hMSCs). Their effects on *in vitro* chondrogenic differentiation and *in vivo* cartilage tissue regeneration were investigated.

4.3 Materials and methods

4.3.1 In vitro 3D culture of hMSCs in collagen scaffolds and measurement of cell seeding efficiency

Scaffold discs cut into cylindrical discs (diameter: 3 mm and thickness: 3 mm) were used for 3D cell culture. After sterilization with 70% ethanol aqueous solution and three washes with PBS, the disc samples were washed once with DMEM. Silicone frames with holes were used to protect cell leakage during cell seeding. The holes had a diameter of 6 mm and a thickness of 4 mm. The silicone frames were placed in a cell culture dish. After the DMEM in each scaffold disc was removed, the scaffold discs were placed in the holes of the silicone frame. The subcultured hMSCs (P4, Lonza, Walkersville, USA) were harvested by trypsinization, and a suspension solution of hMSCs was prepared (5×10^6 cells mL^{-1}). MSCGM™ (Lonza, Walkersville, USA) was used as the culture medium, and the cultivation atmosphere was 5% CO_2 and 37 °C. The cell solution was added to the scaffold discs in the silicone holes (100 μL/scaffold disc) and cultured for 6 h. Then, the medium in the disc samples was removed, and the scaffold discs were turned over. Another 100 μL of cell solution was placed on the scaffold discs. The total cell number seeded on each disc was 1×10^6 cells. After the second cell seeding, the disc samples remained in the silicone holes for an additional 6 h of incubation. After 6 h of incubation, the cell/scaffold discs were removed from the silicone frame, placed in T-flasks, and continually cultivated in serum-containing DMEM (10% fetal bovine serum) for 1 d. Dynamic cultivation at a shaking speed of 60 rpm was performed. The remaining cells in the culture dish and silicone frames (unattached cells) were collected and counted, and this information was used for the calculation of cell seeding efficiency (n=3). After 1 d of culture, the samples were washed once with

DMEM, and the cultivation medium was changed to chondrogenic induction medium, which was high-glucose DMEM supplemented with L-glutamine (4 mM), proline (0.4 mM), nonessential amino acids (0.1 mM), ascorbic acid (50 mg mL^{-1}), dexamethasone (10^{-7} M), TGF-β3 (10 ng ml^{-1}) and 1% ITS. The samples were cultivated in chondrogenic induction medium for 2 w, and the medium was changed every 3 d.

4.3.2 Investigation of adhesion, distribution and viability of hMSCs in collagen scaffolds

After 1 d of cultivation in T flasks, cell/scaffold constructs were fixed with 4% paraformaldehyde for 2 h at RT. After fixation, the samples were washed with pure water, dehydrated and lyophilized. Cells adhered to the scaffolds were observed by SEM.

Nuclear staining was conducted to examine hMSC distribution in the scaffolds. After 1 d of cultivation, the samples were washed and immersed in neutral buffered formalin (10%) for 24 h at RT to fix the cells. After hydration, paraffin embedding, cutting into 7 μm-thick slices and deparaffinization, staining with 4',6-diamidino-2-phenylindole dihydrochloride (DAPI, 1 μg mL^{-1}, 10 m) was conducted. A fluorescence microscope was used to observe the stained slices.

The viability of hMSCs after cultivation in scaffolds for 1 d was evaluated by live/dead staining. After two washes with PBS, the samples were incubated with calcein-AM- and propidium iodide-containing serum-free DMEM for 15 min at 37 °C. The stained cell/scaffold constructs were examined with confocal laser scanning microscopy.

4.3.3 In vivo subcutaneous implantation

Approval for animal experiments was obtained from the animal experiment ethical committee of the National Institute for Materials Science. All experiments were conducted under the institute guidelines. The hMSCs (1×10^6 cells/scaffold) were cultivated in collagen scaffolds in chondrogenic induction medium for 2 w before implantation. Nude mice obtained from Charles River Laboratories (Yokohama, Japan) were used for subcutaneous implantation of the samples. After subcutaneous implantation on the backs of the mice for 2 w, the implants were collected, and their gross appearance was examined by optical microscopy. The size of the harvested implants (n=6) was measured.

4.3.4 Measurements of DNA amount, sulfated glycosaminoglycan (sGAG) amount and mechanical strength

After *in vitro* cultivation for 1 d and 2 w and *in vivo* implantation for 2 w, the samples were washed and lyophilized. Papain solution was used to digest the lyophilized samples by incubation at 60 °C under shaking for 6 h. The papain solution contained μg/mL papain in 0.1 M PBS buffer, L-cysteine hydrochloride monohydrate (5 mM) and EDTA (5 mM). The solution pH was 6. The DNA and sGAG amount in the digestion solution was quantified with Hoechst 33258 and a Blyscan™ Glycosaminoglycan Assay Kit, respectively. Mechanical compression testing was applied to the samples after 2 w of *in vitro* cultivation and implants after 2 w of implantation to measure the Young's modulus of compression. Triplicate samples were used for these measurements.

4.3.5 Real-time PCR

After *in vitro* cultivation for 2 w and *in vivo* implantation for 2 w, the samples were washed and placed in liquid nitrogen for freezing. Pulverization of the frozen samples with an electric crusher was conducted to obtain the powers of each sample. After digestion of the pulverized samples with Sepasol-RNA I Super G solution (1 mL), extraction of total RNA was performed according to the reported protocol [40]. After reverse transcription with a high-capacity cDNA reverse transcription kit, amplification of glyceraldehyde-3-phosphate dehydrogenase (GAPDH, a housekeeping gene), collagen I (Col1a2), collagen II (Col2a1), aggrecan (Acan), SOX9 and collagen X (Col10a1) was conducted with a QuantStudio® 3 Real-Time PCR System (Thermo Fisher Scientific). The primer and probe sequences were as previously reported [40-42]: GAPDH: (forward) 5'-ATGGGGAAGGTGAAGGTCG-3′, (reverse) 5′-TAAAAGCAGCCCTGGTGACC-3′, (probe) 5′-CGCCCAATACGACCAAATCCGTTGAC-3′; collagen type I: (forward) 5′-CAGCCGCTTCACCTACAGC-3′, (reverse): 5′-TTTTGTATTCAATCACTGTCTTGCC-3′, (probe): 5′−CCGGTGTGACTCGTGCAGCCATC-3′; collagen type II: (forward) 5′GGCAATAGCAGGTTCACGTACA-3′, (reverse) 5′-CGATAACAGTCTTGCCCCACTT-3′, (probe) 5′−CCGGTATGTTTCGTGCAGCCATCCT-3′; aggrecan: (forward) 5′-TCGAGGACAGCGAGGCC-3′, (reverse) 5′-TCGAGGGTGTAGCGTGTAGAGA-3′, (probe) 5′-ATGGAACACGATGCCTTTCACCACGA-3′; Sox9: (forward) 5′-CACACAGCTCACTCGACCTTG-3′, (reverse) 5′-TTCGGTTATTTTTAGGATCATCTCG-3′, (probe) 5′-CCCACGAAGGGCGACGATGG-3′; collagen type X: (forward) 5′-CAAGGCACCATCTCCAGGAA-3′, (reverse) 5′-AAAGGGTATTTGTGGCAGCATATT-3′, (probe) 5′-TCCCAGCACGCAGAATCCATCTGA-3′. A $2^{-\Delta\Delta Ct}$ method was used to calculate the relative expression of each gene with an endogenous control (GAPDH). The expression level of each gene by the P4 hMSCs was used for normalization of the gene expression by the cells in the samples. Triplicate samples were used for these analyses.

4.3.6 Histological and immunohistochemical staining

After *in vitro* culture for 2 w and *in vivo* implantation for 2 w, the samples were stained. After 3 washes with PBS and fixation with 10% neutral buffered formalin for 24 h at RT, dehydration, and embedding in paraffin, 7 μm-thick slices were prepared. The slices were stained with hematoxylin/eosin (HE) and safranin O/light green. The slices were also immunohistochemically stained by incubation with antibodies against collagen II, collagen I and aggrecan as previously reported [39]. The stained slices were observed with optical microscopy.

4.3.7 Statistics

Statistical analysis of all the quantitative data was conducted by one-way analysis of variance (ANOVA) using KyPlot 5.0 (KyensLab Inc., Tokyo, Japan). The data are shown as the mean ± standard deviation (S.D.). * ($p < 0.05$), ** ($p < 0.01$) and *** ($p < 0.001$) are used to indicate significant differences.

4.4 Results

4.4.1 Cell seeding efficiency, cell adhesion, distribution and viability

The hMSCs were seeded and cultivated in the collagen scaffolds. More than 95% of the cells were successfully seeded in all the scaffolds (Table 4.1). All the scaffolds had almost the same level of seeding efficiency. The use of a silicone frame during cell seeding could constrain the cell suspension solution and cells in the frame holes, therefore allowing most of the seeding cells to adhere to the scaffolds.

Cell adhesion, distribution and viability were investigated after 1 d of cultivation. SEM observation showed that hMSCs showed good adhesion to all the scaffolds (Fig. 4.1a). Nuclear staining with DAPI showed a homogeneous cell distribution in the PLGA-templated collagen scaffolds and a nonhomogeneous distribution in the control collagen scaffold (Fig. 4.1b). More cells were located on the surface of the control collagen scaffold. In particular, the collagen scaffolds prepared with the PLGA-10-355 sponge template showed the most homogeneous cell distribution. The homogeneous cell distribution can be attributed to the good interconnectivity of PLGA-templated collagen scaffolds. Live/dead staining showed that almost all the hMSCs were stained alive (green fluorescence) in all scaffolds, indicating high cell viability (Fig. 4.1c).

Table 4.1 Cell seeding efficiency (mean ± S.D., n=3).
There was no significant difference among the groups.

Scaffold	Cell seeding efficiency (%)
Control	95.8 ± 2.1
Col-10-150	96.4 ± 0.9
Col-10-250	96.7 ± 0.5
Col-10-355	95.9 ±1.4

4.4.2 Gross appearance and mechanical properties of in vitro cultured cell/scaffold constructs and in vivo implants

The hMSCs were cultured *in vitro* in collagen scaffolds for 2 weeks and implanted *in vivo* for 2 weeks. After *in vitro* culture for 2 weeks, the cell/scaffold constructs were white and soft (Fig. 4.2a). The constructs were slightly shrunken from the size of the scaffolds (Table 4.2). The Young's modulus increased after hMSCs were cultivated in all collagen scaffolds for 2 w (Fig. 4.2b). The Young's modulus of constructs generated in the PLGA-templated collagen scaffolds was significantly higher than that generated in the control.

After 2 w of implantation, the implants were hard and looked reddish (Fig. 4.2a). The reddish color can be attributed to infiltration by blood cells. The implant showed 6~10% shrinkage (Table 4.2). The Young's modulus further increased after implantation for 2 weeks (Fig. 4.2b). The Young's modulus of all implants after 2 weeks of implantation increased to approximately 3.5 times the value before implantation. The implants regenerated in the PLGA-templated collagen scaffolds showed higher Young's modulus values than the implants generated in the control scaffold. The implant generated in the Col-10-355 scaffold had the highest Young's modulus.

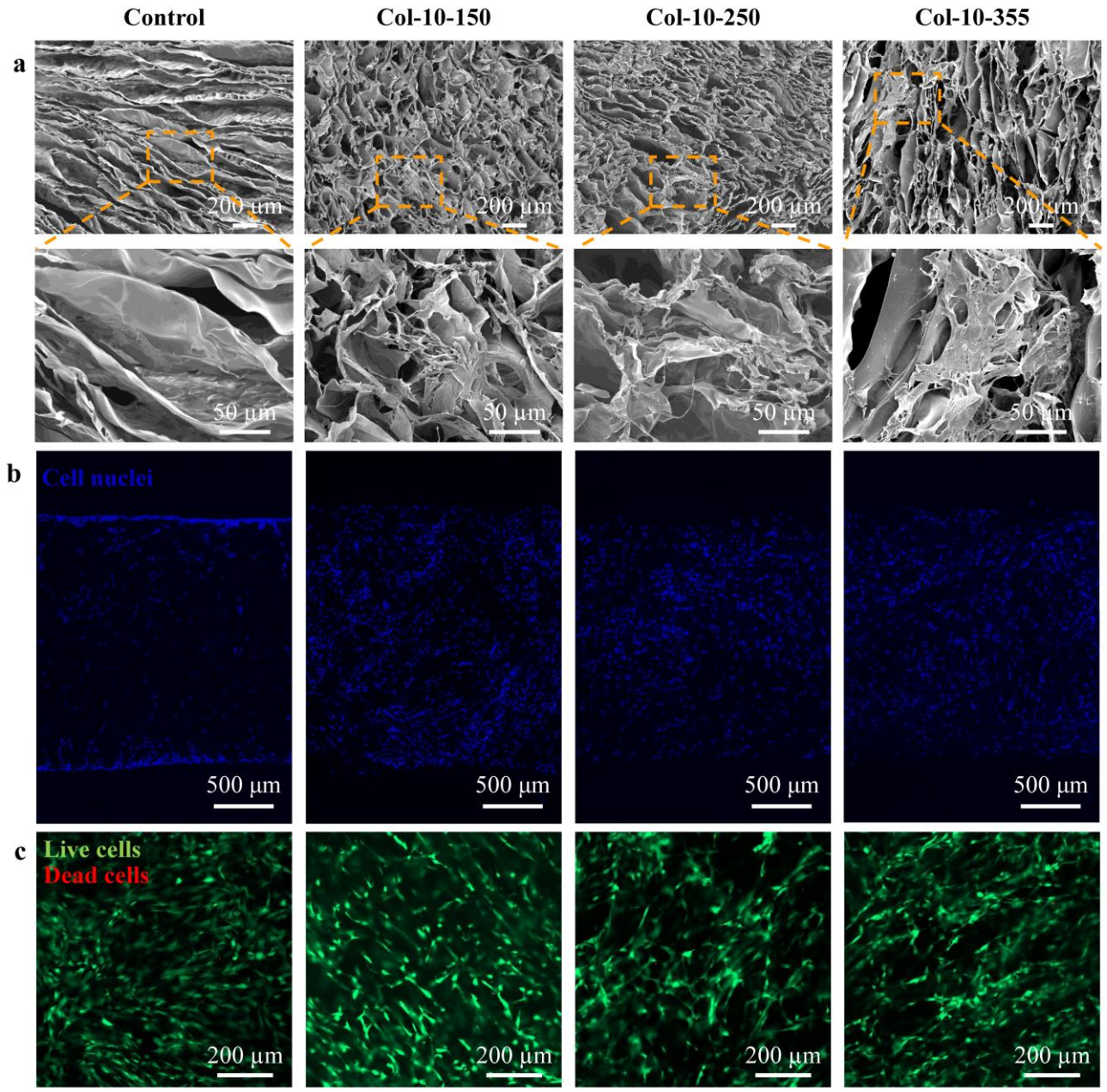

Figure 4.1 (a) SEM images, (b) nuclear staining and (c) live/dead staining of hMSCs cultivated in different scaffolds for 1 d. Blue dots indicate the stained nuclei. Green and red fluorescence indicate live and dead cells, respectively.

4.4.3 DNA and sGAG amounts in cultivated samples and implants

The amount of DNA and sGAG was measured after *in vitro* culture for 1 d and 2 w and after *in vivo* implantation for 2 w (Fig. 4.3). The DNA amounts in all the scaffolds increased with cultivation and implantation time (Fig. 4.3a). At each time point, the DNA amounts in all the scaffolds were not significantly different. These results indicated that the cells could proliferate both on the scaffold surface and in the scaffold pores. The contents of sGAG also increased with cultivation and implantation (Fig. 4.3b). The cells produced

more sGAG in the PLGA-templated collagen scaffolds than in the control. The hMSCs in Col-10-355 showed the highest sGAG amount after 2 w of *in vitro* culture and 2 w of *in vivo* implantation.

The ratio of sGAG/DNA increased after *in vitro* culture and *in vivo* implantation. (Fig. 4.3c). The ratio of sGAG/DNA in the Col-10-355 scaffold showed a significantly greater increase than that in the control collagen scaffold or in Col-10-150 after 2 w of *in vitro* culture. After *in vivo* implantation for 2 w, the sGAG/DNA ratios in the Col-10-150 and Col-10-355 collagen scaffolds were significantly higher than that in the control collagen scaffold. These results suggested that all the scaffolds supported hMSC proliferation and promoted ECM production. The collagen scaffolds fabricated with PLGA sponges showed a higher promotion effect than the control collagen scaffold. The Col-10-355 collagen scaffolds showed the highest promotive effect.

Table 4.2 Table 2 Size of cell/scaffold constructs after 2 weeks of in vitro culture and of implants after 2 weeks of in vivo implantation (mean ±S.D., n=3). There was no significant difference among the groups.

Time point	Control (mm)	Col-10-150 (mm)	Col-10-250 (mm)	Col-10-355 (mm)
Vitro 2W	5.9 ± 0.1	6.0 ± 0.1	5.8 ± 0.1	5.9 ± 0.1
Vivo 2W	5.4 ± 0.3	5.5 ± 0.4	5.6 ± 0.2	5.6 ± 0.2

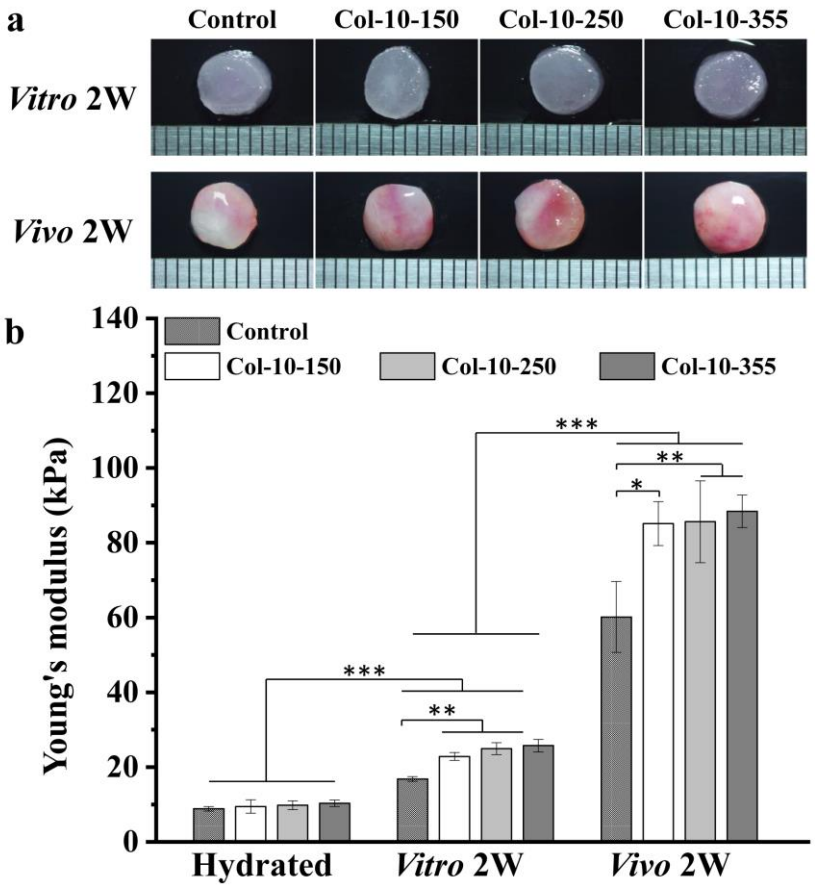

Figure 4.2 (a) Gross appearance and (b) Young's modulus values of samples after hMSCs were cultivated in the scaffolds for 2 w and of implants after 2 w of in vivo implantation. The Young's modulus values of the wet scaffolds are shown for comparison. Data are shown as the mean ± SD, n = 3. Significant difference: *, p

< 0.05; **, p < 0.01; ***, p < 0.001.

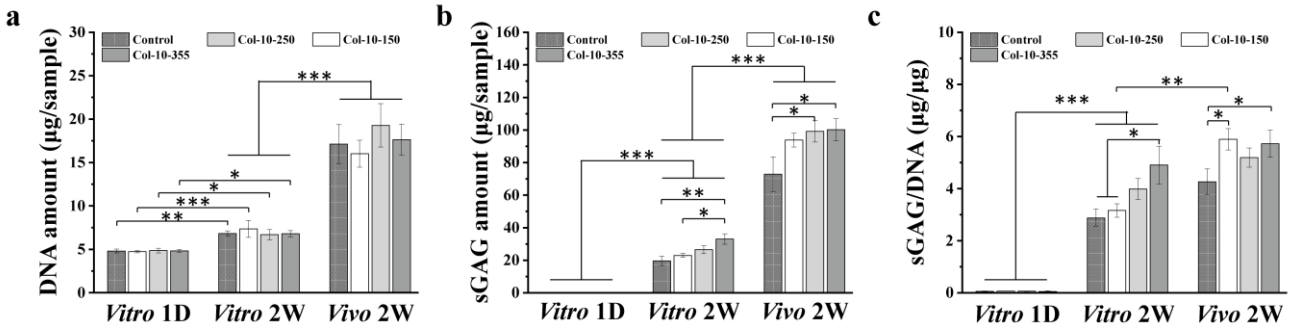

Figure 4.3 Quantification of (a) DNA amount, (b) sGAG amount and (c) sGAG to DNA ratio in the cultivated samples after in vitro cultivation for 1 d and 2 w and in the implants after in vivo implantation for 2 w. Data are shown as the mean ± SD, n = 3. Significant difference: *, p < 0.05; **, p < 0.01; ***, p < 0.001.

4.4.4 Expression of cartilaginous genes

Aggrecan and collagen II are two markers of hyaline cartilage. SOX9 is a key transcription factor of chondrogenesis. Collagen X is a chondrocyte hypertrophy marker. Collagen I is a fibrous cartilage marker. The expression of genes encoding these markers was analyzed after hMSCs were cultured *in vitro* for 2 w and implanted *in vivo* for 2 w (Fig. 4.4). The genes encoding collagen II, aggrecan, SOX9 and collagen X genes of hMSCs in all the collagen scaffolds were upregulated after culturing in chondrogenic induction medium for 2 w. However, the expression level of collagen I decreased after 2 w of cultivation in chondrogenic induction medium. The expression levels of collagen II and SOX9 decreased after 2 w of *in vivo* implantation. The expression levels of aggrecan and collagen X were almost the same before and after *in vivo* implantation, except for the expression of collagen X in the Col-10-150 scaffold. In contrast, the expression level of collagen I increased after *in vivo* implantation for 2 weeks. Among all the collagen scaffolds, the control collagen scaffold group showed the highest expression of collagen I. The cells in the Col-10-355 collagen scaffold showed the highest expression of collagen II, aggrecan and SOX9.

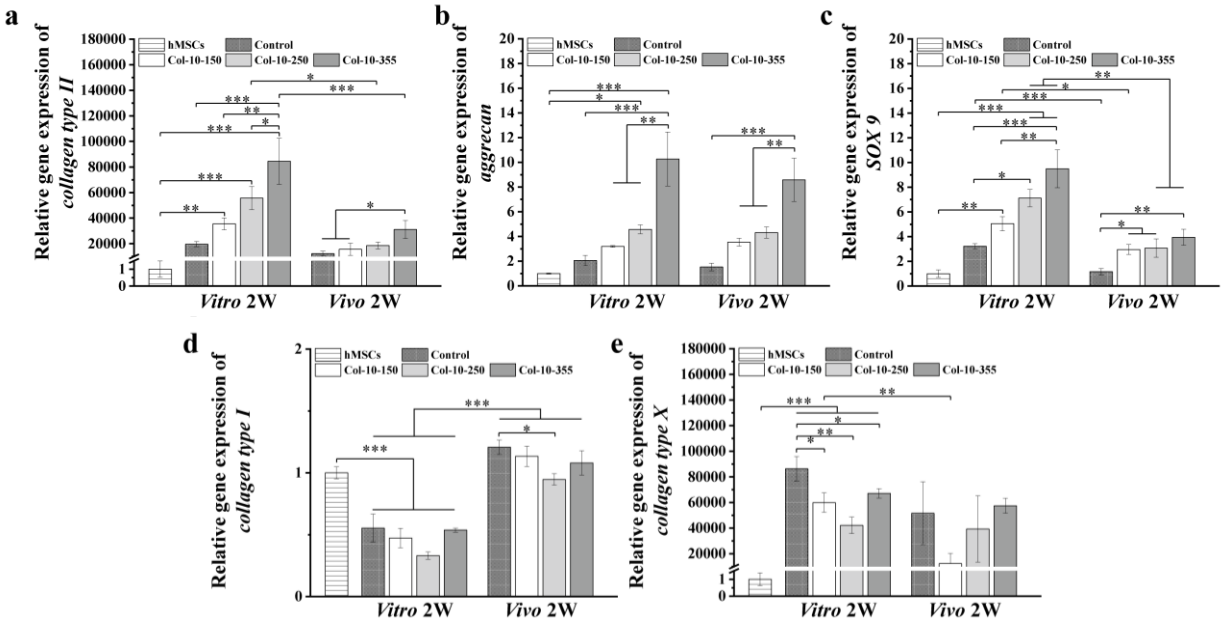

Figure 4.4 Expression of genes encoding (a) collagen II, (b) aggrecan, (c) SOX9, (d) collagen I and (e) collagen X of P4 hMSCs and hMSCs cultivated in vitro in collagen scaffolds for 2 w and implants after 2 w of implantation. The expression of each gene was normalized to that of the P4 hMSCs. Data are shown as ± SD, n = 3. Significant difference: *, $p < 0.05$; **, $p < 0.01$; ***, $p < 0.001$.

4.4.5 Histological and immunohistochemical staining results

The *in vitro* cell/scaffold constructs and *in vivo* implants were stained with HE and safranin O (Fig. 4.5). HE staining showed homogeneous cell and extracellular matrix distribution in the PLGA-templated collagen scaffolds. However, some void spaces were observed in the control. All the collagen scaffolds showed stronger staining of the extracellular matrix after 2 w of *in vivo* implantation compared with the *in vitro* cultivated constructs. Safranin O staining also showed a homogeneous distribution of cartilaginous extracellular matrices in the PLGA-templated collagen scaffolds. Immunohistochemical staining of collagen II showed dense staining in all the collagen scaffolds after 2 weeks of *in vivo* implantation. Collagen II and aggrecan showed a more homogeneous distribution in the PLGA-templated scaffold than in the control. Among all the PLGA-templated collagen scaffolds, the Col-10-355 scaffold showed the strongest staining of aggrecan and collagen II. Collagen I was weakly stained in the PLGA-templated collagen scaffolds. In contrast, it was strongly stained in the control. The streaks observed in the control collagen scaffold can be attributed to the cells and matrices on the pore walls of the control collagen scaffold. More cells were present on the surface, and fewer cells were distributed in the inner pores of the control collagen scaffold, as shown in Fig. 3b. The nonhomogeneous cell distribution resulted in the formation of void spaces that were observed as streaks in the staining images. The histological and immunohistochemical staining results indicated that the PLGA-templated collagen scaffolds were beneficial for articular cartilage matrix secretion and homogeneous distribution.

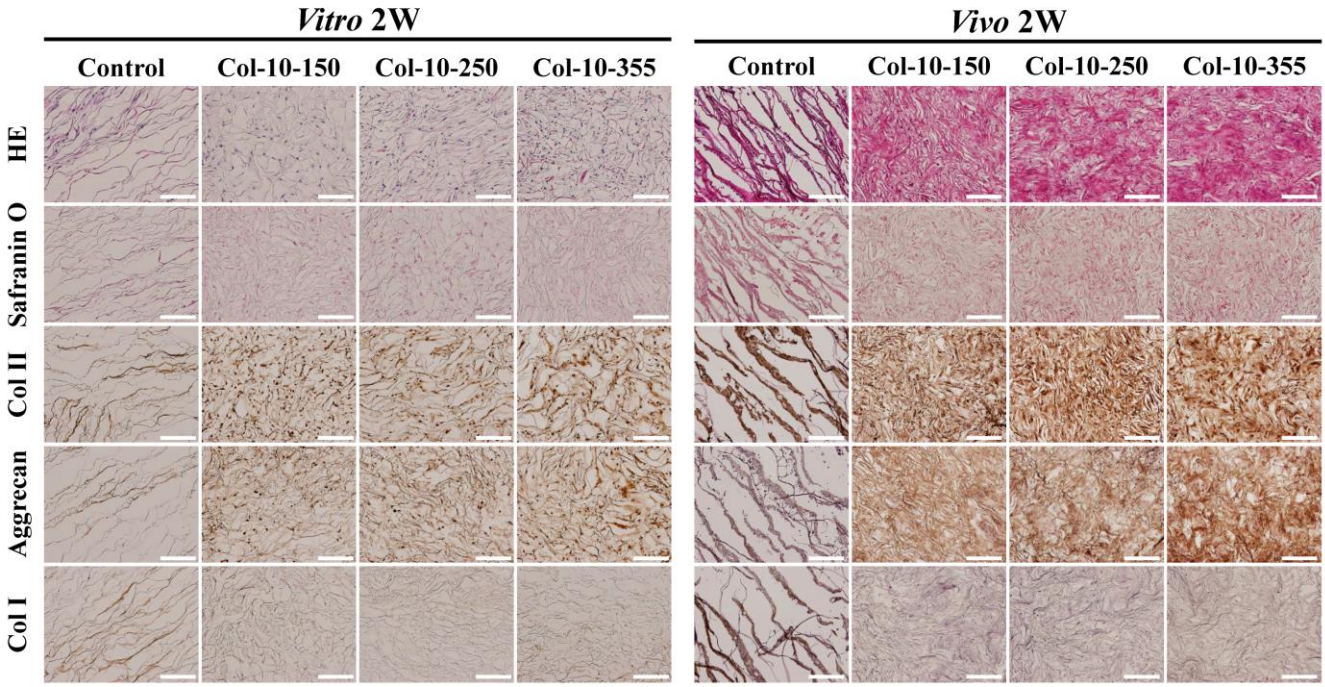

Figure 4.5 Photomicrographs of HE staining, safranin O staining and immunohistochemical staining of collagen II, aggrecan and collagen I after hMSCs were cultivated in vitro in the scaffolds for 2 w or implanted for 2 w. Scale bar = 200 μm.

4.5 Discussion

The culture of hMSCs in 3D porous scaffolds has attracted broad attention for cartilage regeneration. The 3D porous scaffolds can help to accommodate hMSCs homogeneously to accelerate cell–cell interactions for chondrogenic differentiation. Moreover, chondrogenic induction factors such as dexamethasone and TGF-β3 are required to promote the chondrogenic differentiation of hMSCs [43]. Accordingly, here, collagen scaffolds with high interconnectivity were fabricated and used for the 3D cultivation of hMSCs. The channels in the PLGA-templated collagen scaffolds showed beneficial effects on homogeneous hMSC distribution throughout the scaffolds. The cells cultivated in the PLGA-templated collagen scaffolds showed higher expression of cartilaginous genes, higher secretion of cartilaginous matrices and higher Young's modulus values than those cultivated in the control scaffold. *In vivo* implantation further showed cell proliferation and the production of cartilage-related matrices, consequently increasing the Young's modulus. Specifically, the Col-10-355 collagen scaffold showed the highest promotive effect, which can be attributed to its large interconnecting channels that could facilitate cell migration, homogeneous cell distribution and cell–cell interaction more strongly throughout the scaffold. Interconnected pore structures have beneficial effects on chondrogenic differentiation [44, 45].

The cell/scaffold constructs were cultivated in chondrogenic induction medium supplemented with dexamethasone and TGF-β3. Dexamethasone and TGF-β3 have been reported to stimulate chondrogenesis and regulate chondrogenic genes [46, 47]. Chondrogenesis-related genes, such as collagen type II, aggrecan and SOX9, were upregulated after 2 weeks of *in vitro* culture in chondrogenic induction medium. The PLGA-templated collagen scaffolds showed higher expression levels of chondrogenesis genes, especially the Col-10-355 scaffold. The beneficial pore structure for cell–cell interaction, together with the chondrogenic induction factors, should stimulate the chondrogenic differentiation of hMSCs in the PLGA-templated collagen scaffolds more strongly than in the control. After *in vivo* implantation, the expression of the genes encoding collagen II, aggrecan and SOX9 decreased, which can be attributed to the use of chondrogenic induction factors during *in vitro* culture but not during *in vivo* implantation. Although 2 w of *in vitro* culture could significantly promote cartilaginous gene expression, the withdrawal of chondrogenic induction factors could affect the expression of these genes. Continual delivery of chondrogenic induction factors should be considered even after *in vivo* implantation to further promote the chondrogenic differentiation of hMSCs.

The implants generated in the PLGA-templated collagen scaffolds showed stronger mechanical properties than those generated in the control. In particular, the Col-10-355 scaffold showed the highest promotive effect. The more homogeneous distributions of cells ECM and the higher secretion of cartilaginous matrices in the PLGA-templated collagen scaffolds should enhance the mechanical properties of regenerated cartilage tissue. The PLGA-templated collagen scaffolds, especially the Col-10-355 scaffold, would be useful for the 3D cultivation of hMSCs for cartilage regeneration.

4.6 Conclusions

The PLGA-templated collagen scaffolds were applied for the 3D cultivation of hMSCs for chondrogenic differentiation and cartilage tissue regeneration. The PLGA-templated collagen scaffolds facilitated homogeneous cell distribution and supported cell adhesion and proliferation. They promoted the expression of cartilaginous genes and the production of cartilage-related matrices. After *in vivo* implantation, the PLGA-templated collagen scaffolds, especially the Col-10-355 scaffold, further promoted cartilaginous gene and

matrix expression. Tissue regenerated in the Col-10-355 scaffold had the highest Young's modulus. The highly interconnected collagen scaffolds facilitated the hMSC chondrogenesis and cartilage regeneration.

4.7 References

[1] Y. Campos, A. Almirall, G. Fuentes, H.L. Bloem, E.L. Kaijzel, L.J. Cruz, Tissue Engineering: An Alternative to Repair Cartilage, Tissue Engineering Part B: Reviews 25(4) (2019) 357-373.
[2] E.A. Makris, A.H. Gomoll, K.N. Malizos, J.C. Hu, K.A. Athanasiou, Repair and tissue engineering techniques for articular cartilage, Nat Rev Rheumatol 11(1) (2015) 21-34.
[3] W. Wei, H. Dai, Articular cartilage and osteochondral tissue engineering techniques: Recent advances and challenges, Bioactive materials 6(12) (2021) 4830-4855.
[4] L. Nimeskern, G.J.V.M. van Osch, R. Müller, K.S. Stok, Quantitative Evaluation of Mechanical Properties in Tissue-Engineered Auricular Cartilage, Tissue Engineering Part B: Reviews 20(1) (2013) 17-27.
[5] M. Anderson-Baron, M. Kunze, A. Mulet-Sierra, A.B. Adesida, Effect of cell seeding density on matrix-forming capacity of meniscus fibrochondrocytes and nasal chondrocytes in meniscus tissue engineering, The FASEB Journal 34(4) (2020) 5538-5551.
[6] A.S. Croft, S. Illien-Jünger, S. Grad, J. Guerrero, S. Wangler, B. Gantenbein, The Application of Mesenchymal Stromal Cells and Their Homing Capabilities to Regenerate the Intervertebral Disc, International journal of molecular sciences 22(7) (2021).
[7] I. Urlić, A. Ivković, Cell Sources for Cartilage Repair—Biological and Clinical Perspective, Cells 10(9) (2021).
[8] W. Kabir, C. Di Bella, I. Jo, D. Gould, P.F.M. Choong, Human Stem Cell Based Tissue Engineering for In Vivo Cartilage Repair: A Systematic Review, Tissue Engineering Part B: Reviews 27(1) (2020) 74-93.
[9] E.D. Aldrich, X. Cui, C.A. Murphy, K.S. Lim, G.J. Hooper, C.W. McIlwraith, T.B.F. Woodfield, Allogeneic mesenchymal stromal cells for cartilage regeneration: A review of in vitro evaluation, clinical experience, and translational opportunities, STEM CELLS Translational Medicine 10(11) (2021) 1500-1515.
[10] L. Peterson, H.S. Vasiliadis, M. Brittberg, A. Lindahl, Autologous Chondrocyte Implantation: A Long-term Follow-up, The American Journal of Sports Medicine 38(6) (2010) 1117-1124.
[11] E.M. Darling, K.A. Athanasiou, Rapid phenotypic changes in passaged articular chondrocyte subpopulations, Journal of Orthopaedic Research 23(2) (2005) 425-432.
[12] R.F. Canadas, R.P. Pirraco, J.M. Oliveira, R.L. Reis, A.P. Marques, Stem Cells for Osteochondral Regeneration, in: J.M. Oliveira, S. Pina, R.L. Reis, J. San Roman (Eds.), Osteochondral Tissue Engineering: Challenges, Current Strategies, and Technological Advances, Springer International Publishing, Cham, 2018, pp. 219-240.
[13] B.D. Markway, G.-K. Tan, G. Brooke, J.E. Hudson, J.J. Cooper-White, M.R. Doran, Enhanced Chondrogenic Differentiation of Human Bone Marrow-Derived Mesenchymal Stem Cells in Low Oxygen Environment Micropellet Cultures, Cell Transplantation 19(1) (2010) 29-42.
[14] R. Kuroda, K. Ishida, T. Matsumoto, T. Akisue, H. Fujioka, K. Mizuno, H. Ohgushi, S. Wakitani, M. Kurosaka, Treatment of a full-thickness articular cartilage defect in the femoral condyle of an athlete with autologous bone-marrow stromal cells, Osteoarthritis and Cartilage 15(2) (2007) 226-231.
[15] S. Wakitani, T. Mitsuoka, N. Nakamura, Y. Toritsuka, Y. Nakamura, S. Horibe, Autologous Bone Marrow Stromal Cell Transplantation for Repair of Full-Thickness Articular Cartilage Defects in Human Patellae: Two Case Reports, Cell Transplantation 13(5) (2004) 595-600.
[16] H. Madry, A. Rey-Rico, J.K. Venkatesan, B. Johnstone, M. Cucchiarini, Transforming Growth Factor Beta-Releasing Scaffolds for Cartilage Tissue Engineering, Tissue Engineering Part B: Reviews 20(2) (2013) 106-125.
[17] M. Zhu, W. Zhong, W. Cao, Q. Zhang, G. Wu, Chondroinductive/chondroconductive peptides and their-functionalized biomaterials for cartilage tissue engineering, Bioactive materials 9 (2022) 221-238.
[18] R. Chijimatsu, M. Kobayashi, K. Ebina, T. Iwahashi, Y. Okuno, M. Hirao, A. Fukuhara, N. Nakamura, H. Yoshikawa, Impact of dexamethasone concentration on cartilage tissue formation from human synovial derived stem cells in vitro, Cytotechnology 70(2) (2018) 819-829.
[19] B. Grigolo, G. Lisignoli, A. Piacentini, M. Fiorini, P. Gobbi, G. Mazzotti, M. Duca, A. Pavesio, A. Facchini, Evidence for redifferentiation of human chondrocytes grown on a hyaluronan-based biomaterial (HYAFF®11): molecular, immunohistochemical and ultrastructural analysis, Biomaterials 23(4) (2002) 1187-1195.
[20] M.M.J. Caron, P.J. Emans, M.M.E. Coolsen, L. Voss, D.A.M. Surtel, A. Cremers, L.W. van Rhijn, T.J.M. Welting, Redifferentiation of dedifferentiated human articular chondrocytes: comparison of 2D and 3D cultures, Osteoarthritis and Cartilage 20(10) (2012) 1170-1178.
[21] B.A.G. Melo, Y.A. Jodat, S. Mehrotra, M.A. Calabrese, T. Kamperman, B.B. Mandal, M.H.A. Santana,

E. Alsberg, J. Leijten, S.R. Shin, 3D Printed Cartilage‐Like Tissue Constructs with Spatially Controlled Mechanical Properties, Advanced Functional Materials 29(51) (2019).
[22] H. Kwon, W.E. Brown, C.A. Lee, D. Wang, N. Paschos, J.C. Hu, K.A. Athanasiou, Surgical and tissue engineering strategies for articular cartilage and meniscus repair, Nat Rev Rheumatol 15(9) (2019) 550-570.
[23] Q. Zhang, H. Lu, N. Kawazoe, G. Chen, Pore size effect of collagen scaffolds on cartilage regeneration, Acta Biomaterialia 10(5) (2014) 2005-13.
[24] S. Chen, Q. Zhang, N. Kawazoe, G. Chen, Effect of high molecular weight hyaluronic acid on chondrocytes cultured in collagen/hyaluronic acid porous scaffolds, RSC Advances 5(114) (2015) 94405-94410.
[25] S. Chen, Q. Zhang, T. Nakamoto, N. Kawazoe, G. Chen, Gelatin Scaffolds with Controlled Pore Structure and Mechanical Property for Cartilage Tissue Engineering, Tissue Eng Part C Methods 22(3) (2016) 189-98.
[26] K. Lin, D. Zhang, M.H. Macedo, W. Cui, B. Sarmento, G. Shen, Advanced Collagen-Based Biomaterials for Regenerative Biomedicine, Advanced Functional Materials 29(3) (2019).
[27] H. Lu, Y.G. Ko, N. Kawazoe, G. Chen, Cartilage tissue engineering using funnel-like collagen sponges prepared with embossing ice particulate templates, Biomaterials 31(22) (2010) 5825-35.
[28] A.J. Lausch, L.C. Chong, H. Uludag, E.D. Sone, Multiphasic Collagen Scaffolds for Engineered Tissue Interfaces, Advanced Functional Materials 28(48) (2018).
[29] V. Irawan, T.-C. Sung, A. Higuchi, T. Ikoma, Collagen scaffolds in cartilage tissue engineering and relevant approaches for future development, Tissue engineering and regenerative medicine 15(6) (2018) 673-697.
[30] S. Marlovits, S. Aldrian, B. Wondrasch, L. Zak, C. Albrecht, G. Welsch, S. Trattnig, Clinical and Radiological Outcomes 5 Years After Matrix-Induced Autologous Chondrocyte Implantation in Patients With Symptomatic, Traumatic Chondral Defects, The American Journal of Sports Medicine 40(10) (2012) 2273-2280.
[31] M.-H. Zheng, C. Willers, L. Kirilak, P. Yates, J. Xu, D. Wood, A. Shimmin, Matrix-Induced Autologous Chondrocyte Implantation (MACI®): Biological and Histological Assessment, Tissue engineering 13(4) (2007) 737-746.
[32] M. Marcacci, M. Berruto, D. Brocchetta, A. Delcogliano, D. Ghinelli, A. Gobbi, E. Kon, L. Pederzini, D. Rosa, G.L. Sacchetti, G. Stefani, S. Zanasi, Articular Cartilage Engineering with Hyalograft® C: 3-Year Clinical Results, Clinical Orthopaedics and Related Research® 435 (2005).
[33] G. Lutzweiler, J. Barthes, G. Koenig, H. Kerdjoudj, J. Mayingi, F. Boulmedais, P. Schaaf, W. Drenckhan, N.E. Vrana, Modulation of Cellular Colonization of Porous Polyurethane Scaffolds via the Control of Pore Interconnection Size and Nanoscale Surface Modifications, ACS Appl Mater Interfaces 11(22) (2019) 19819-19829.
[34] Y. Liu, J.-H. Kim, D. Young, S. Kim, S.K. Nishimoto, Y. Yang, Novel template-casting technique for fabricating β-tricalcium phosphate scaffolds with high interconnectivity and mechanical strength and in vitro cell responses, Journal of Biomedical Materials Research Part A 92A(3) (2010) 997-1006.
[35] S. Reed, G. Lau, B. Delattre, D.D. Lopez, A.P. Tomsia, B.M. Wu, Macro-and micro-designed chitosan-alginate scaffold architecture by three-dimensional printing and directional freezing, Biofabrication 8(1) (2016) 015003.
[36] K. Qin, C. Parisi, F.M. Fernandes, Recent advances in ice templating: from biomimetic composites to cell culture scaffolds and tissue engineering, Journal of Materials Chemistry B 9(4) (2021) 889-907.
[37] S. Li, F. Tallia, A.A. Mohammed, M.M. Stevens, J.R. Jones, Scaffold channel size influences stem cell differentiation pathway in 3-D printed silica hybrid scaffolds for cartilage regeneration, Biomater Sci 8(16) (2020) 4458-4466.
[38] M. Rasoulianboroujeni, N. Kiaie, F.S. Tabatabaei, A. Yadegari, F. Fahimipour, K. Khoshroo, L. Tayebi, Dual Porosity Protein-based Scaffolds with Enhanced Cell Infiltration and Proliferation, Scientific Reports 8(1) (2018) 14889.
[39] Y. Xie, K. Lee, X. Wang, T. Yoshitomi, N. Kawazoe, Y. Yang, G. Chen, Interconnected collagen porous scaffolds prepared with sacrificial PLGA sponge templates for cartilage tissue engineering, Journal of Materials Chemistry B 9(40) (2021) 8491-8500.
[40] K. Lee, Y. Chen, X. Li, N. Kawazoe, Y. Yang, G. Chen, Influence of viscosity on chondrogenic differentiation of mesenchymal stem cells during 3D culture in viscous gelatin solution-embedded hydrogels, Journal of Materials Science & Technology 63 (2021) 1-8.
[41] H. Lu, T. Hoshiba, N. Kawazoe, I. Koda, M. Song, G. Chen, Cultured cell-derived extracellular matrix scaffolds for tissue engineering, Biomaterials 32(36) (2011) 9658-9666.
[42] D. Raghothaman, M.F. Leong, T.C. Lim, J.K.C. Toh, A.C.A. Wan, Z. Yang, E.H. Lee, Engineering cell

matrix interactions in assembled polyelectrolyte fiber hydrogels for mesenchymal stem cell chondrogenesis, Biomaterials 35(9) (2014) 2607-2616.
[43] N. Indrawattana, G. Chen, M. Tadokoro, L.H. Shann, H. Ohgushi, T. Tateishi, J. Tanaka, A. Bunyaratvej, Growth factor combination for chondrogenic induction from human mesenchymal stem cell, Biochemical and Biophysical Research Communications 320(3) (2004) 914-919.
[44] J.M. Kemppainen, S.J. Hollister, Differential effects of designed scaffold permeability on chondrogenesis by chondrocytes and bone marrow stromal cells, Biomaterials 31(2) (2010) 279-87.
[45] J. Zhang, Y. Wu, T. Thote, E.H. Lee, Z. Ge, Z. Yang, The influence of scaffold microstructure on chondrogenic differentiation of mesenchymal stem cells, Biomedical Materials 9(3) (2014) 035011.
[46] H. Tanaka, C.L. Murphy, C. Murphy, M. Kimura, S. Kawai, J.M. Polak, Chondrogenic differentiation of murine embryonic stem cells: Effects of culture conditions and dexamethasone, Journal of Cellular Biochemistry 93(3) (2004) 454-462.
[47] Q.O. Tang, K. Shakib, M. Heliotis, E. Tsiridis, A. Mantalaris, U. Ripamonti, E. Tsiridis, TGF-β3: A potential biological therapy for enhancing chondrogenesis, Expert Opinion on Biological Therapy 9(6) (2009) 689-701.

Chapter 5

General conclusions

This dissertation describes a method to prepare collagen scaffolds with interconnected porous structure for the application of cartilage tissue engineering.

Chapter 1 provides a general introduction of current treatments of articular cartilage defects and their limitations. Furthermore, the functions of porous scaffold in tissue engineering are outlined and fabrication methods are summarized. In order to solve the current problems of preparation methods, the objective and outline are defined.

Chapter 2 describes the preparation process of PLGA templates using solvent casting and particulates leaching method. Collagen scaffolds with interconnected porous structures were obtained by using PLGA sponges as templates. The interconnecting channels were formed in the collagen scaffolds after selectively leaching PLGA templates. These collagen scaffolds, in particular the Col-10-355 scaffold, had high interconnectivity with large interconnecting channels throughout the scaffolds.

Chapter 3 describes the 3D culture of bovine articular chondrocytes in the collagen scaffolds. Chondrocytes showed homogenous distribution, fast proliferation, high expression of cartilaginous genes and high secretion of cartilaginous extracellular matrix in the collagen scaffolds. In particular, the collagen scaffold templated by the PLGA sacrificial sponge that was prepared with a high weight ratio of PLGA and large salt particulates showed the most promotive effect on cartilage tissue formation. The interconnected pore structure facilitated cell distribution, cell-cell interaction and cartilage tissue regeneration.

Chapter 4 describes the chondrogenic differentiation of human bone marrow-derived mesenchymal stem cells in collagen scaffolds both *in vitro* and *in vivo*. The hMSCs attached and distributed homogenously in these scaffolds, showed high proliferation and expression level of chondrogenesis genes and production of cartilage-related matrix. After *in vivo* implantation, these collagen scaffolds, especially the Col-10-355 scaffold, further promoted cell proliferation and regeneration of cartilage-like tissue. Tissue regenerated in the Col-10-355 scaffold had the highest Young's modulus. The highly interconnected collagen scaffolds facilitated the chondrogenesis of hMSCs and cartilage regeneration.

In conclusion, PLGA sponges with different pore size and porosities were used to prepare collagen scaffold with interconnected porous structures. The PLGA-templated collagen scaffolds benefited homogenous distribution, fast proliferation, high expression of cartilaginous genes and high secretion of cartilaginous extracellular matrix when chondrocytes were cultured in the scaffolds. Furthermore, the scaffolds could promote chondrogenic differentiation of hMSCs. The PLGA sponge template method is a good method for preparation of interconnected collagen scaffolds. The interconnected collagen scaffold should be useful for cartilage tissue engineering.

List of publications

1. **Yan Xie**, Kyubae Lee, Xiuhui Wang, Toru Yoshitomi, Naoki Kawazoe, Yingnan Yang, Guoping Chen. Interconnected collagen porous scaffolds prepared with sacrificial PLGA sponge templates for cartilage tissue engineering. Journal of Materials Chemistry B. 2021,9, 8491-8500.

2. **Yan Xie**, Naoki Kawazoe, Yingnan Yang, Guoping Chen. Preparation of Mesh-like Collagen Scaffolds for Tissue Engineering. Materials Advances. 2022, 3, 1556-1564.

3. **Yan Xie**, Linawati Sutrisno, Toru Yoshitomi, Naoki Kawazoe, Yingnan Yang, Guoping Chen. Three-dimensional culture and chondrogenic differentiation of mesenchymal stem cells in collagen scaffolds with high interconnectivity. Submitted to Biomedical Materials.

4. **Yan Xie**, Jing Zheng, Linawati Sutrisno, Naoki Kawazoe, Yingnan Yang, Guoping Chen. Synergistic effect of chondrogenesis inductive factor and scaffold structure on chondrogenic differentiation of mesenchymal stem cells. In preparation.

Acknowledgements

First and foremost, I would like to express my sincere gratitude to my supervisor Professor Guoping Chen. He has helped me a lot from the beginning when I took the entrance examination of University of Tuskuba. During Ph.D course, he has devoted himself to supervise my research, such as how to design research topic, how to carry out experiments, how to solve the problems. His profound knowledge, unique insight and creative spirit in scientific research have greatly encouraged me. He gives valuable insight to me to let me think more deeply about my research. He is not only my supervisor in research but also a lifelong mentor. I really appreciate that Professor Chen has accepted me as his student to do research at his lab. My experience here and the things I learned from him will be the greatest treasure in my life.

I would like to express my special gratitude to Dr. Naoki Kawazoe for his kind help and guidance. His immense knowledge, professional skill, and modest character have deeply impressed me. Whenever I need any help, he is always so kind to help me to solve the problems. I am very grateful to work with him and learn from him.

I also would like to thank Dr. Toru Yoshitomi for his support and encouragement. He gives me many valuable suggestions that help me a lot. I am so pleasure to work with him.

I really appreciate the valuable suggestion and assistance from Dr. Yingjun Yang, Dr. Xiuhui Wang, Dr. Yazhou Chen, Dr. Kyubae Lee, Dr. Yongtao Wang, Ms. Linawati Sutrisno, Mr. Jing Zheng, Mr. Huajian Chen and Mr. Rui Sun. They help me a lot in research and daily life.

I also want to express my sincere appreciation to Mrs. Akiyama Haruyo and Mrs. Akiko Ito. They assist me with a lot of paperwork and procedures related to NIMS and University of Tsukuba. Their sincere efforts bring great convenience to me.

I would like to thank my thesis committee members, Professor Yukio Nagasaki, Professor Tetsushi Taguchi and Professor Kohsaku Kawakami for their insightful comments, encouragement and meaningful suggestions during my PhD pre-defense and final defense.

I would like to give my most sincere thanks to my families and my friends. No matter what happened, they've always been there to back me up.

This work was performed at Tissue Regeneration Materials Group of Research Center for Functional Materials (RCFM) in National Institute for Materials Science (NIMS) and Graduate School of Pure and Applied Science of University of Tsukuba. I appreciate the financial support from NIMS Junior Research Assistantship.